Climate Immobility in Sub-Saharan Africa

Édouard Pignède Julien Wolfersberger*

Abstract

Migration is widely recognized as a key mechanism for adapting to climate change. However, in many developing countries, liquidity constraints limit households' ability to migrate in response to climate shocks, resulting in spatial misallocations of labor that hinder economic development. This paper quantifies the economic costs of these misallocations. Using reduced-form estimations, we start by documenting heterogeneity in migration response to drought according to the income level, which is consistent with the liquidity constraint hypothesis. Then, we develop a quantitative spatial model of migration and trade by combining satellite and census data. We find that, by 2080, 31 million potential migrants will be trapped by climate change and that this leads to substantial welfare losses across African economies. Our results further highlight how liquidity constraints amplify the spatial heterogeneity in the impacts of climate change across and within countries of the region.

Keywords: Climate Change; Migration; Adaptation; Development
JEL codes: F18; O13; Q10; Q54; Q56; R12

*Pignède and Wolfersberger: Paris-Saclay University, AgroParisTech and Climate Economics Chair of Paris-Dauphine.
We thank Raja Chakir, Bruno Conte, Philippe Delacote and Christophe Gouel for helpful comments and discussions. We also want to thank the participants of the following seminars where this work was presented: DIAL, UNU-WIDER ; and of those conferences: Paris-Saclay Conference on Trade and Environment, EAERE.

1 Introduction

Developing countries have experienced significant increases in the frequency and intensity of climate extremes in recent decades, with future temperature rises expected to exceed the global average (Ranasinghe et al. 2021). Migration, as a response to changing weather conditions, has historically served as an adaptation strategy across diverse contexts (Berlemann and Steinhardt 2017; Borderon et al. 2019). However, climate-induced shocks often erode household resources, constraining their ability to migrate and leaving them caught in a "climate trap", increasingly exposed to environmental hazards.

In this paper, we build a rich quantitative model to study the cost of immobility caused by climate change in Sub-Saharan Africa (SSA). As the marginal returns to economic activity in space change with new climate conditions, reallocating workers across sectors and locations is a key mechanism for the economy to adapt. However, in many regions of the developing world, workers face liquidity constraints that may not allow them to move freely. These populations are effectively "trapped" in locations exposed to worsening climate conditions, generating aggregate frictions that we call spatial misallocations. In this paper, we quantify the resulting welfare losses from the failure to reallocate labor efficiently in response to climate shocks.

Our results show the sizable impact of labor misallocation between and within countries of SSA. We find that climate change increases the number of trapped workers by 31 million, and this liquidity constraints increase welfare losses due to climate change by 0.8 percentage points in 2080. We show that there are critical differences across countries.

We first present a set of motivations for our quantitative model. Using district-level data on migration rates, we examine how climate shocks impact migration in SSA, conditionally on income. Our results show that an increase in the number of droughts tends to increase the probability of migration only for individuals who have a higher level of education. To the extent that education is correlated with income, we interpret this result as evidence of the presence of a liquidity constraint within districts and between households. Furthermore, we show that droughts also decrease long-distance migrations (i.e., more than 300km) for almost all individuals except for the richest ones. These results hold using a long-differences specification over several decades.

Having documented these immobility facts, we build a quantitative spatial model of migration and trade to quantify their welfare cost. This is critical since this immobility likely hampers development and poverty reduction in regions of the world that will experience the most dramatic impacts of climate change. Building on the recent literature on quantitative

spatial models (Redding and Rossi-Hansberg 2017), we consider an economy divided between many locations, each composed of a continuum of plots. There are two sectors in our model: agriculture and an outside sector representing a composite of industry and services. In agriculture, the use of each plot is determined by the highest land rental rate between crops. This implies that farmers allocate each plot to the crop that provides the highest returns according to an exogenous distribution of land productivity, which is itself subject to climate change. The outside sector employs labor only, and productivity in this sector can also be affected by temperatures. Workers display idiosyncratic tastes in location, and migration across both locations and sectors is costly. Finally, trade between locations is subject to iceberg costs, a key feature of the African economy.

The main insights from the model are the following. To adapt to new climate conditions, workers can choose to migrate or change their working sector depending on expected wages elsewhere, the cost of moving between location-sectors, and the liquidity constraint they face. Their ability to incur the cost of migrating depends on the unequal income distribution across space and the local impacts of climate change. Regarding production, farmers can choose to grow different crops or extend the amount of land used to face changes in local prices. This choice depends on their location's productivity and labor cost, which depend on climate conditions and migration. Finally, as the relative price of agricultural goods to the outside goods changes under new climate conditions, a given location might also trade differently.

Central to our modeling framework, we introduce mobility frictions due to liquidity constraints in each location-sector pair. Given the distribution of these frictions, workers incur an upfront cost to migrate towards a desirable location. Relative to standard models of migration, this cost is not only a linear function of the distance between locations, but it also depends on total income in a given location. It follows that workers cannot move to *all* locations but only to those where their liquidity allows it. Another critical feature of our framework is the inclusion of costs associated with moving labor across sectors. Drawing on the extensive literature addressing the agricultural productivity gap (Gollin et al. 2013), our model incorporates a wedge affecting labor returns in the non-agricultural sector.

To calibrate the model, we estimate migration costs by fitting precise data on migration flows in 2005 and 2010 (Ceausu et al. 2021). By adopting this approach, we find costs that are substantially higher than those in previous papers, relying mostly on distance measures. This is because we are able to capture other crucial aspects of migration, such as language barriers, and thus obtain arguably more precise estimates. For the calibration of the other components of the model, we take advantage of the FAO-GAEZ data on potential yields for a large set of crops under different climate scenarios. We also use satellite data on

urbanization, distribution of economic activities, and population repartition to inform the non-agricultural sector, as well as initial and predicted population endowments.

Equipped with our model, we implement the following counterfactual exercises. In the first step, we simulate the spatial equilibrium of the economy in 2080 in *absence of climate change* and with future population size at the origin. This allows us to derive predicted migrations induced by demographic changes in 2080 in SSA. In a second step, we simulate the outcome of the economy in 2080 with population growth but also *with climate change*, precisely under the RCP8.5 scenario (provided by the GAEZ project). This corresponds to the most pessimistic climate scenario, which we interpret as an upper bound of our model predictions if no actions were taken to reduce global GHG emissions. We then identify immobility as the number of workers who do not migrate with the resource constraint but would have migrated without it.

Our findings highlight how climate change further reinforces resource-constrained immobility. Under an RCP8.5 scenario, 31 million additional workers are trapped relative to a no-climate-change scenario. The inclusion of such resource-constrained mobility increases global welfare loss due to climate change by 0.8 percentage points. Our findings also suggest an important movement of urbanization. We further describe the strong heterogeneity of this immobility across districts and sectors, and how the inclusion of this immobility constraint redistributes the spatial impact of climate change.

This paper is related to several strands of the literature. The papers closest to ours use quantitative spatial models to study questions related to climate change, including migration. This is the case of Conte (2022), who also focuses on SSA and studies how new climate conditions will impact the movement of workers by 2080. Our contribution is to introduce budget mobility constraints and quantify the social cost of the impossibility of reallocating labor across region-sector pairs. This is important in order not to overestimate adaptation capacities. Other recent works closely related to ours include Cruz and Rossi-Hansberg (2021), Burzyński et al. (2022) or Desmet and Rossi-Hansberg (2023). While these papers also adopt a similar methodology to study the impacts of climate change, they do not focus on the role of resource constraints faced by households, as we do here.

Another strand of papers focuses on international trade and studies how climate change affects adaptation in the agricultural sector (Costinot et al. 2016; Conte et al. 2021; Gouel and Laborde 2021). While our framework allows for adaptation through trade both within and between countries, we depart from these works by allowing for another adaptation channel, which is crucial in the context of SSA: migration.

Our work is also connected to the large empirical literature studying the impact of climate shocks on different development outcomes, such as migrations (e.g., Henderson et al. 2017; Colmer 2021; Hoffmann et al. 2024) or inequalities (Pignède 2025). The first part of our analysis, assessing empirically how global warming affects emigration within African countries, is especially connected to those works. We differ by a key aspect, though, as our empirical strategy is rather designed to highlight heterogeneity in the probability of leaving a given location. By doing that, our work is related to that of Cattaneo and Peri (2016) and Peri and Sasahara (2019), who document lower mobility among the poorest but do so at the country level, not within the country as we do here. Another key aspect is that, unlike the second part of this paper, those works do not incorporate a model of migration and trade to quantify the costs of immobility under different scenarios.

Finally, this work also speaks to the papers that have examined the role of liquidity constraints on the probability of migrating in the context of RCTs (Millán et al. 2020; Gazeaud et al. 2023) or by exploiting rich census and survey data (Bazzi 2017; Clemens and Mendola 2024). Overall, these works point to the fact that negative income shocks tend to lower migration, with the latter viewed as a costly human capital investment. Our paper contributes to this literature by studying the role of climate change as a negative income shock with spatially heterogeneous responses.

The rest of the paper is organized as follows. Section 2 documents empirical facts motivating our approach. In section 3, we lay out the model and take it to the data in section 4. Our results are shown in section 5, and section 6 concludes.

2 Empirical motivations

This section is articulated in three parts. First, we study the causal impact of droughts on migration rates across African districts. Second, we look at how these weather shocks affect the distances of migration. In the third part, we focus on long-term climate trends instead of short-term shocks. Each time, we highlight heterogeneous responses conditional on income level, proxied by education.

2.1 Migration responses to droughts

In this section, we want to assess the migration response to climate shocks from individuals with different income levels, which we proxy using the level of education. To do this, we

use census data from 21 countries of SSA and work at the first administrative level within each of these countries (i.e., district level).[1]

We restrict our analysis to the push factor of bad weather events, such as agricultural droughts, that negatively impact the revenue of agricultural households. Formally, we estimate the following gravity model:

$$M_{ijt} = \beta D_{i[t-10,t]} + \phi_{ij} + \gamma_{jt} + \epsilon_{ijt}, \tag{1}$$

where our dependent variable, M_{ijt}, is the migration rate from district i to district j at year t for individuals with different levels of education: less than primary, primary, secondary, or tertiary school completion. The variable $D_{i[t-10,t]}$ is the number of droughts, weighted by district area affected, experienced by district i in the previous ten years. We voluntarily consider a long-time period to take into account the cumulative impact of weather shocks on migration (Di Falco et al. 2024), and better align with our model that examines climate change's long-term effects on migration. A drought is experienced when the mean of the 6-month SPEI falls below -1 during the year t (Zhou et al. 2023).[2] The term ϕ_{ij} designates origin and destination fixed-effects to account for migration frictions between i and j that do not vary over time, such as distance between locations, language, or ethnicity barriers. The term γ_{jt} is a destination-year fixed-effect, accounting for pull factors that drive migration from a destination. These include variations in wages or climate conditions at the destination.

We estimate the model for individuals of different levels of education. The underlying assumption is that the level of education is correlated with their income. As a result, low-educated individuals may be more prone to drought-induced liquidity constraints that impede them from migrating. We leave results using alternative indexes, as well as other weather covariates, in Appendix B.

Figure 1 presents the estimates of the β coefficient from equation (1). We present three specifications with different sets of fixed effects. While all the models control for origin-destination confounding factors, the third one is more demanding as it accounts for every destination-year unobserved shock. These may include climate or economic shocks that would facilitate or hinder migration from individuals at origin, given their characteristics.

Across the three specifications, the results show that the lower the level of education is, the less likely migration is to occur. To the extent that education is correlated with income, migration is limited by liquidity constraints in locations facing a negative climate shock. For

1. We use census data from IPUMS, which can be accessed at https://international.ipums.org/. To save space, we describe the database and provide additional results in Appendix B.

2. Resuts with other definitions of drought are given in Appendix B, Table B.1

Figure 1: Elasticity of migration in response to drought events

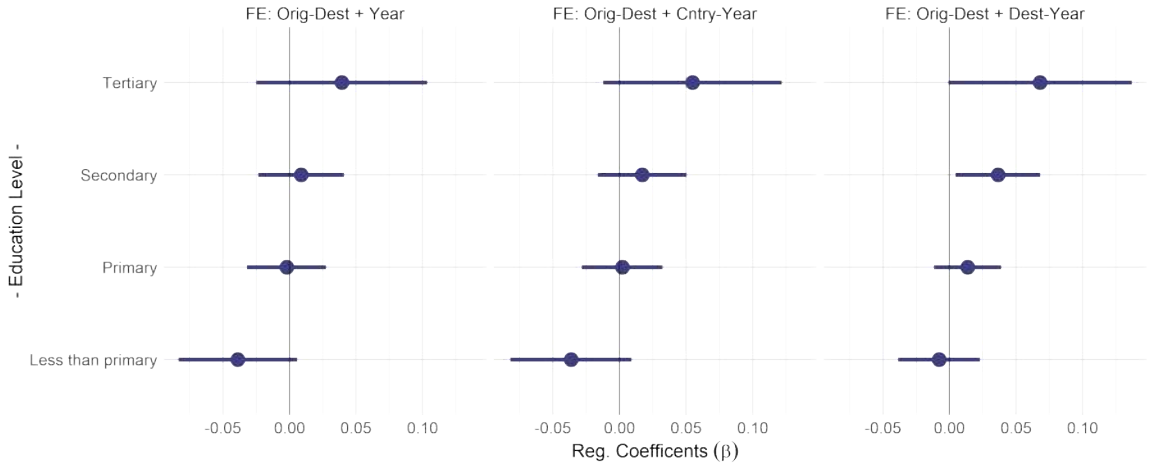

Note: Coefficient of regression β from equation 1 with different level time-varying fixed-effects. Error bars represent a 95% confidence interval. Droughts are defined as the number of years in the last ten years where the 6-month SPEI went below -1.

instance, in the more demanding model, one additional drought has no significant effect on migration for the "less than primary" educated category. At the same time, it significantly increases the probability of individuals from secondary and tertiary education migrating.

We are not the first ones to uncover such results. Our findings are related to previous studies, such as Cattaneo and Peri (2016), Cattaneo et al. (2019), or Hoffmann et al. (2024) more recently. Overall, it suggests that adaptation through migration seems to be a strategy only available to highly educated individuals. This result is likely due to the severe resource constraints faced by the low-educated individuals.

2.2 Impact of drought on the distance migration

The scenario of a liquidity constraint limiting the movement of individuals implies a diminution of long-distance migrations when shocks impact households' income. To test this hypothesis, we build on the previous model, adding an interaction between the drought indicator and the migration distance between i and j, $Dist_{ij}$. Formally, we estimate the following model for all individuals:

$$M_{ijt} = \beta D_{i[t-10,t]} \times Dist_{ij} + \phi_{ij} + \gamma_{jt} + \epsilon_{ijt}, \tag{2}$$

Table 1 shows the heterogeneity of the impact of drought on bilateral migration according to the distance between districts. Results show that droughts significantly lower migration by more than 300 kilometers for all households except the richest ones. This result is in line

Table 1: Migration elasticity for different level of migration distance

Dependent Variable:	Migration rate (log)							
Education	Less than primary		Primary		Secondary		Tertiary	
	(1)	(2)	(3)	(4)	(5)	(6)	(7)	(8)
Variables								
Droughts	-0.008	0.004	0.014	0.020	0.036**	0.042**	0.068*	0.066*
	(0.016)	(0.017)	(0.013)	(0.013)	(0.016)	(0.017)	(0.035)	(0.036)
Droughts × Distance > 300 km		-0.223***		-0.144**		-0.173**		0.051
		(0.072)		(0.066)		(0.086)		(0.169)
Observations	11,630	11,630	11,253	11,253	9,773	9,773	6,617	6,617
Mean dep. var.	0.004	0.004	0.006	0.006	0.010	0.010	0.015	0.015
Mean mig. dist.	204.0	204.0	225.1	225.1	258.5	258.5	279.6	279.6

Note: Results of regression of equation 2 using Poisson maximum likelyhood estimator. Origin-destination and destination-year fixed-effects are included in all regressions. Droughts are defined as the number of years in the last ten years where the 6-month SPEI went below -1. 300 kilometers is the median distance between two districts in the datasets.

with a mechanism of liquidity constraint that impedes the poorest households from moving to costly destinations, using the distance of migration as a proxy for migration costs.[3]

2.3 Long-term impact of climate on migration

The two previous sections show how individuals migrate due to weather shocks (here, agricultural droughts). It shows that only more educated households move and that migration distance is decreased. We now look at the long-term impact of climate on internal migration.

To do so, we use a long-differences specification (Dell et al. 2014) to measure how migrations evolved following long-term changes in local climate conditions. That is, we compare the mean changes in bilateral migrations when individuals face higher increases in mean temperature or in drought frequency. We estimate the following model by levels of education:

$$\Delta M_{ij} = \beta_{\Delta} \Delta C_i + \gamma_j + \epsilon_{ij}, \tag{3}$$

3. The threshold of 300km was chosen since it is the median distance between the districts of our sample. Robustness with other thresholds is given in Appendix B, Table B.2

where ΔM_{ij} is the difference in mean migration rate between the period 1970-2000 and the period 2000-2020, and ΔC_i is the change in climate indicators (mean temperature and number of droughts) between the same two periods. The term γ_j designates destination fixed-effects to account for pull factors at the destination, and ϵ_{ij} is the error term. Figure 2 presents the results.

Figure 2: Long-term effect of climate on bilateral migration

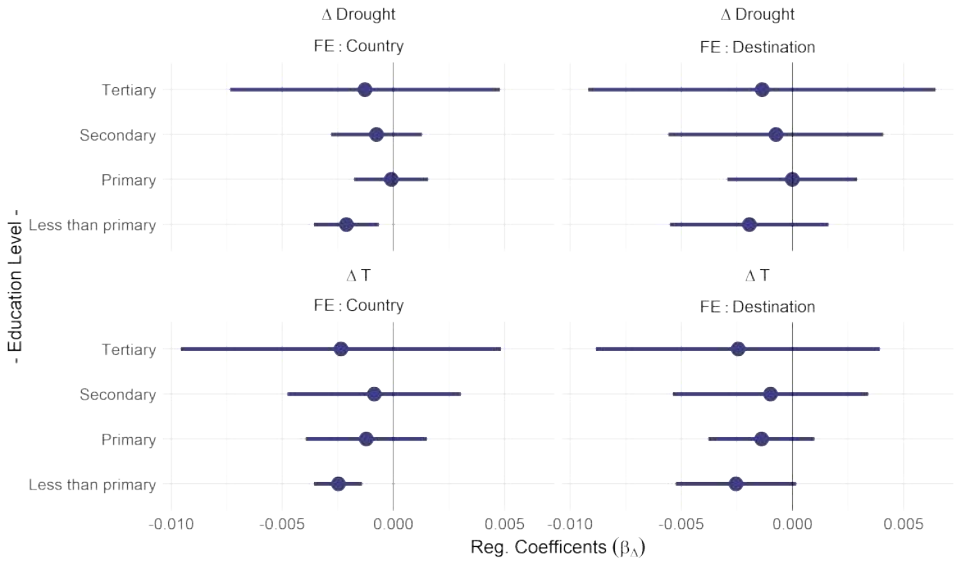

Note: Coefficient of regression β_Δ from equation 3 with different level time-varying fixed-effects. Error bars represent a 95% confidence interval. Droughts are defined as the number of years during which the 6-month SPEI went below -1.

Results show that the migration rate of low-educated households has decreased significantly more in locations more impacted by climate change. These results may be taken cautiously because the number of censuses before the year 2000 is small, as depicted in Figure B.1.

These empirical results challenge the strong impact that climate change ought to have on migration (Rigaud et al. 2018) as frictions of migration and liquidity constraints could play a strong part in impeding such migrations, especially in poor regions of the world with relatively high migration costs, such as SSA.[4]

This "non-adaptation" may imply, in turn, substantial aggregate costs in terms of welfare. As a given location becomes less and less productive due to climate change, liquidity constraints generate spatial misallocations of labor as some households remain "trapped" in non-productive areas. Our goal in this paper is to quantify the costs of these misallocations.

4. For example, Conte (2022) finds that migration frictions in SSA are 50% higher than in Europe.

For this purpose, we build a spatial model of migration and trade that we present in the next section.

3 The model

We consider an economy composed of a set of locations, denoted by $i, j \in \mathcal{L}$. In each location, it is possible to grow crops $k \in \{1, \ldots, K\} = A$, or to produce a manufacturing good M. We view the latter as a composite good of industry and services. Each location has a land area ϕ_i composed of a continuum of plots ω used to grow crop k. The set of all goods in the economy is noted $\mathcal{G} = A \cup M$. Workers supply labor inelastically and rent land to producers, who redistribute the rent to the local population.

Shipping goods from i to j is subject to iceberg transport costs $\kappa_{ij} = (d_{ij})^{\delta}(1 + \tau_{ij})$, where d_{ij} is the shortest bilateral distance between the two locations and τ_{ij} is an additional positive tariff-like trade friction which is null if i and j belong to the same country. In our model, migration is costly across locations and sectors. Workers moving from location-sector ik to location-sector js incur a cost m_{ik}^{js}.

3.1 Production and land-use

Agricultural production. Production of a crop $k \in A$ combines land and labor as follows:

$$Q_i^k(\omega) = z_i^k(\Lambda_i^k(\omega)\phi_i^k(\omega))^{\alpha_k}\left(N_i^k(\omega)\right)^{1-\alpha_k} \tag{4}$$

where ϕ_i^k and $N_i^k(\omega)$ denote respectively land-use and labor employed to produce crop k. The parameter z_i^k is the total factor productivity, which accounts for the level of technology as well as local working conditions. The parameter $0 < \alpha^k < 1$ is the share of land intensity, and $\Lambda_i^k(\omega)$ is a plot-specific land productivity factor. We assume that $\Lambda_i^k(\omega)$ is randomly distributed from a Fréchet distribution with parameters $\{\gamma A_i^k, \theta\}$:

$$P(\Lambda_i^k(\omega) < z) = \exp\left\{-\left(\frac{z}{\gamma A_i^k}\right)^{-\theta}\right\},$$

where $\gamma = \frac{1}{\Gamma(1-1/\theta)}$, Γ being the Gamma function, and $E[\Lambda_i^k(\omega)] = A_i^k$ is the unconditional average yield of crop k in location i. The parameter θ controls the dispersion of agricultural productivity across land plots within a location i. High values of θ imply less heterogeneity in land productivity.

In each location $i \in \mathcal{L}$, producers maximize profits by choosing between crops $k \in \mathcal{K}$ given wage w_i^A and land rental $r_i^k(\omega)$ rates. This yields the following land rent for each plot $\omega \in \Omega_i$:

$$r_i^k(\omega) = r_i^k \Lambda_i^k(\omega), \text{ with } r_i^k = \left(\tilde{\alpha} \frac{p_i^k}{(w_i^A)^{1-\alpha_k}} \right)^{\frac{1}{\alpha_k}}. \tag{5}$$

From the land rent expression, we can see that the economic value of any given plot in the economy is the product of its exogenous land productivity, $\Lambda_i^k(\omega)$, and a profitability index denoted by r_i^k. The latter increases with market price $p_i^k \; \forall k \in \mathcal{G}$, decreases with the cost of labor w_i, and is a function of a constant $\tilde{\alpha} = (\alpha_k)^{\alpha_k}(1-\alpha_k)^{(1-\alpha_k)}$.[5]

Exploiting the distributional assumption of the land productivity parameter, $\Lambda_i^k(\omega)$, yields the following land use allocation in each region i:

$$\pi_i^k = \frac{(r_i^k A_i^k)^\theta}{\sum\limits_{k' \in \mathcal{G}} (r_i^{k'} A_i^{k'})^\theta}. \tag{6}$$

Equation (6) explains land-use allocation between goods by the relative profitability of each of these goods. This profitability is the product of an economic term r_i^k and a location-specific parameter A_i^k. For agricultural goods, this parameter represents soil quality and climate conditions. In our counterfactual exercise, we exploit differences in A_i^k according to climate scenarios to understand how changes in productivity affect migration flows.

The value of production of a good $k \in \mathcal{G}$, for any region $i \in \mathcal{L}$, is given by:

$$X_i^k = \frac{1}{\alpha_k} r_i^k \phi_i A_i^k (\pi_i^k)^{(\theta-1)/\theta}, \tag{7}$$

where ϕ_i is total land area in region i. Again, the role of A_i^k in defining comparative advantages between locations is straightforward here. From (6) and (7), the model predicts that those with a higher drawn A_i^k will produce more good k and allocate more land to it.

Manufacturing production. Production of the manufacturing good M requires only labor and is given by:

$$Q_i^M = z_i^M N_i^M, \tag{8}$$

where z_i^M is the total factor productivity of the manufacturing sector and N_i^M is the labor employed in this sector. First-order conditions imply that the wage in the manufacturing sector is equal to the marginal product of labor, $w_i^M = p_i^M z_i^M$, and that the total value of production of the manufacturing good is given by $X_i^M = w_i^M N_i^M$.

5. The derivations of the model are provided in Appendix C.

3.2 Preferences, location, and consumption

The utility of a worker moving from the location i and working in sector k to the location j and the sector s is denoted:

$$U_{ik}^{js} = \frac{C_{js}}{m_{ik}^{js}} \epsilon_{js}(\nu), \tag{9}$$

where C_{js} represents consumption, m_{ik}^{js} is the utility cost of moving from location i to j and from sector k to s, and $\epsilon_{js}(\nu)$ an idiosyncratic preference shifter that is i.i.d. across locations and workers. The taste parameter $\epsilon_{js}(\nu)$ is assumed to follow a Type-I extreme value distribution (also known as Gumbel distribution) with dispersion ν.

Note that migration costs, m_{ik}^{js}, incorporate frictions to move from sector k to s. This is introduced to account for the agricultural productivity gap between the agricultural and the outside sector (Gollin et al. 2013). It follows that, within the same location, wages in agriculture and manufacturing can differ.

We assume the following form for migration costs: $m_{ik}^{js} = \zeta_{ik}^{js} m_{ik}^{F,js}$, with $m_{ik}^{F,js}$ the financial component of the migration costs, and ζ_{ik}^{js} a factor that incorporates non-financial components of migration costs, such as language barriers (Grogger and Hanson 2011).

Inspired by the work of Marchal and Naiditch (2020), we assume that workers *cannot* migrate to *any* location. Indeed, in each location-sector pair, workers face a liquidity constraint whose distribution is given by Φ. In any location i and sector k, when this liquidity constraint exceeds the cost of migrating to location j and sector s, migration does not occur. This implies that, between the locations of our model, workers not only differ in location tastes but also in financial constraints. Workers move to the utility-maximizing location-sector pair *net* of their liquidity constraint. This feature, critical to the problem we aim to study, is not present in most of the recent papers using similar models and linking climate change and migration (e.g., Cruz and Rossi-Hansberg 2021; Conte 2022).

By exploiting the properties of the Gumbel distribution, it is possible to write the migration rate from location-sector ik to js pairs as:

$$\beta_{ik}^{js} = \sum_{lt=\theta(ik,js)} \left\{ \Phi\left(m_{ik}^{F,\kappa(ik,lt+1)}\right) - \Phi\left(m_{ik}^{F,\kappa(ik,lt)}\right) \right\} \frac{\left(C_{js}\right)^{\nu} \left(m_{ik}^{js}\right)^{-\nu}}{\sum_{j's'=1}^{lt} \left(C_{\kappa(ik,j's')}\right)^{\nu} \left(m_{ik}^{\kappa(ik,j's')}\right)^{-\nu}}, \tag{10}$$

where $\theta(ik, js)$ is the rank of location-sector js when destinations are ordered by migration cost from location-sector ik. The term $\kappa(ik, lt)$ is the inverse permutation.

The first term is the probability that the set of locations available is exactly the first lt least costly destinations. The second term represents the net-utility maximizing location-

sector js. The total population in location j working in the sector s is then given by:

$$N_j^s = \sum_{i \in \mathcal{L}} \sum_{k \in \mathcal{G}} \beta_{ik}^{js} N_{0,i}^k, \tag{11}$$

where $N_{0,i}^k$ designates the initial population in i and sector k.

Without budget constraint, the bilateral migration rate would be:

$$\beta_{ik}^{js,\{\text{NBC}\}} = \frac{(C_{js})^{\nu} (m_{ik}^{js})^{-\nu}}{\sum_{j' \in \mathcal{L}} \sum_{s' \in \mathcal{G}} (C_{j's'})^{\nu} \left(m_{ik}^{j's'}\right)^{-\nu}}, \tag{12}$$

We define the number of trapped workers as the number of people who would have migrated without the budget constraint, but do not. It is equal to:

$$N_{b,i}^k = (\beta_{ik}^{ik} - \beta_{ik}^{ik,\{\text{NBC}\}}) N_{0,i}^k \tag{13}$$

This number is strictly positive as by construction $\beta_{ik}^{ik} \geq \beta_{ik}^{ik,\{\text{NBC}\}}$

For a given good $k \in \mathcal{G}$, consumers in location-sector js value varieties from different origins in an Armington setting such that:

$$C_{js}^k = \left(\sum_{i \in \mathcal{L}} (q_{ij}^k)^{\frac{\eta^k - 1}{\eta^k}} \right)^{\frac{\eta^k}{\eta^k - 1}}, \tag{14}$$

where q_{ij}^k is the quantity of good $k \in \mathcal{G}$ produced in i and consumed in j, and η^k is the Armington elasticity of substitution between varieties. The first-order conditions ensure that the share of consumption spent on good k equals:

$$\lambda_{ij}^k = \left(\frac{p_{ij}^k}{P_j^k} \right)^{1 - \eta^k}, \tag{15}$$

where P_j^k is the Dixit-Stiglitz price index, denoted:

$$P_j^k = \left(\sum_{i \in \mathcal{L}} (p_{ij}^k)^{1 - \eta^k} \right)^{\frac{1}{1 - \eta^k}}. \tag{16}$$

Workers' choice among the $\mathcal{K}$ crops takes a CES form:

$$C_{js}^A = \left(\sum_{k \in \mathcal{K}} (C_{js}^k)^{(\gamma - 1)/\gamma} \right)^{\gamma/(\gamma - 1)}, \tag{17}$$

With γ, the elasticity of substitution between crops. It follows that the share of expenditures on crop k relative to all agricultural goods is:

$$\Xi_j^k = \left(\frac{P_j^k}{P_j^A}\right)^{1-\gamma}, \tag{18}$$

with:

$$P_j^A = \left(\sum_{k\in\mathcal{G}} (P_j^k)^{1-\gamma}\right)^{\frac{1}{1-\gamma}}. \tag{19}$$

Finally, workers' utility features non-homothetic preferences over the consumption of agricultural and non-agricultural goods. Following Comin et al. (2021), we have:

$$\sum_{k\in\{A,M\}} (\Omega_k)^{1/\sigma}(C_{js})^{\epsilon_k/\sigma}(C_{js}^k)^{(\sigma-1)/\sigma} = 1, \tag{20}$$

where σ is the elasticity of substitution between agricultural and non-agricultural sectors, and ϵ_k is their non-homothetic elasticity of substitution. Optimal consumption implies that consumption equals real income in both sectors, such that:

$$C_{js} = \frac{E_j^s}{P_{js}} = \frac{w_j^s + R_j^s/N_j^s}{P_{js}},$$

The share of consumption of aggregate good $k \in \{A, M\}$ relative to total expenditure in location-sector js is then equal to:

$$\mu_{js}^k = \Omega_k \left(\frac{P_j^k}{P_{js}}\right)^{1-\sigma} \left(\frac{E_j^s}{P_{js}}\right)^{\epsilon_k-(1-\sigma)}, \tag{21}$$

with:

$$P_{js} = \left(\sum_{k\in\{A,M\}} (\Omega_k (P_j^k)^{1-\sigma})^{\frac{1-\sigma}{\epsilon_k}} (\mu_{js}^k (E_j^s)^{1-\sigma})^{\frac{\epsilon_k-(1-\sigma)}{\epsilon_k}}\right)^{\frac{1}{1-\sigma}}. \tag{22}$$

Here, P_{js} designates the local price index in location-sector js. Finally, total expenditure in j on a good k imported from i is given by:

$$X_{ij}^k = \lambda_{ij}^k \Xi_j^k \left(\mu_{jA}^A E_j^A N_j^A + \mu_{jM}^A E_j^M N_j^M\right). \tag{23}$$

$$X_{ij}^M = \lambda_{ij}^M \left(\mu_{jA}^M E_j^A N_j^A + \mu_{jM}^M E_j^M N_j^M\right). \tag{24}$$

On the RHS of (23) and (24), the term in parentheses is total spending in j, that is, the sum of income from labor in agriculture, $w_j^A N_j^A$, from labor in the non-agricultural sector, $w_j^M N_j^M$, and from land, $\sum_{k\in\{\mathcal{A},\mathcal{M}\}} R_j^k$.

Lastly, we evaluate the welfare of individuals in location j as the sum of the utility of all agents leaving in j:

$$W_j = \sum_{s\in\{A,M\}} N_j^s \left(\sum_{i\in\mathcal{L}} \sum_{k\in\{A,M\}} \frac{(E_{js}/P_{js})}{m_{ik}^{js}} \right)^{1/\nu} \tag{25}$$

Notice that, by incorporating the moving costs m_{ik}^{js} in the welfare formula, we capture the financial burden of migration, which is the focus of our paper.

We now turn to the clearing conditions of our model and define the equilibrium.

3.3 Market clearing and competitive equilibrium

Clearing conditions for the market of goods impose that the value of production equals that of consumption in any location $i \in \mathcal{L}$ (sum of exports and local consumption):

$$X_i^k = \sum_{j\in\mathcal{L}} \left(\frac{\kappa_{ij} p_i^k}{P_j^k} \right)^{1-\eta_k} \left(\frac{P_j^k}{P_j^A} \right)^{1-\gamma} \left(\mu_{jA}^A E_j^A N_j^A + \mu_{jM}^A E_j^M N_j^M \right). \tag{26}$$

$$X_i^M = \sum_{j\in\mathcal{L}} \left(\frac{\kappa_{ij} p_i^M}{P_j^M} \right)^{1-\eta_M} \left(\mu_{jA}^M E_j^A N_j^A + \mu_{jM}^M E_j^M N_j^M \right). \tag{27}$$

Trade is balanced in every location, so the value of total imports is equal to the value of total exports:

$$\sum_{i\in\mathcal{L}} \sum_{k\in\mathcal{G}} X_{ij}^k = \sum_{i\in\mathcal{L}} \sum_{k\in\mathcal{G}} X_{ji}^k, \tag{28}$$

which can be rewritten as:

$$\sum_{k\in\mathcal{G}} X_i^k = E_j^A N_j^A + E_j^M N_j^M. \tag{29}$$

We can then define a competitive equilibrium as follows:

Definition 1. *Given exogenous parameters $\{\eta_k, \alpha_k, \theta, \nu, m_{ij}, A_i^k, \sigma, z_i^k, \phi_i, \kappa_{ij}\}$, a competitive equilibrium consists of set of prices p_i^k, wage w_i of workers, sectoral rents r_i^k of land, distribution of population N_i, land allocation π_i^k and sectoral production Q_i^k for goods $k \in \mathcal{G}$ and location $i \in \mathcal{L}$ such that equations (5), (6), (7), (11), (16), (19), (21), (22), (26), (27), and (29) hold.*

We now present the empirical quantification of the model.

4 Taking the model to the data

We calibrate our model on a large set of data in SSA, between the years 2005 and 2010. To calibrate the fundamentals of the model, which allow us to recover the initial equilibrium, we invert parts of the model. In this section, we describe the data used to retrieve each parameter, and Appendix C.2 presents the inverted equations in details.

Agricultural yields and production. Our model incorporates a large number of crops. This allows us to consider new channels of adaptation, for example, by allowing the harvesting of new crops that would benefit from new climate conditions. It also allows us to obtain a more accurate mapping of the complex and heterogeneous impacts of climate change on yields.

The GAEZ project provides, for a high number of crops, the grided potential yields, the level of agricultural output, the harvested areas for historical years, as well as potential yields under different climate change scenarios. Since we calibrate the model on African agriculture, we use the rain-fed and low-input data, which better characterize the continent.

For potential yields, A_i^k, we use historical data for the period 1981–2010. Then, we calibrate the local agricultural productivity parameter z_i^k using the data on agricultural production, X_i^k.[6]

For data on crop yields under climate change, we use the RCP8.5 scenario provided by the IPCC. It is considered the most pessimistic scenario, accounting for global average surface warming of 3.7 degrees Celsius at the end of the century.

Rural and urban population. We use data from the Global Human Settlement project (Schiavina, Freire, et al. 2023; Schiavina, Melchiorri, et al. 2023) to retrieve urban and rural populations in all administrative areas. These are high-resolution data on population distribution and urban locations based on both administrative census and satellite data of urban settlements.

We assume that the rural population works in the agricultural sector and the urban population in the outside sector. Given the value of output in each region-sector pair, we can obtain the value of the factor payments w_i^A, w_i^M, and r_i^k.

For the growth in population, we use country-level data projection from United Nations (2022), which models population without migration based on demographic considerations.

6. Data on production, expressed in tonnes, are converted in values using local agricultural GDP data.

Migration costs. To correctly measure household liquidity constraints, it is fundamental to obtain an accurate measure of migration costs faced by households. While the literature has mainly estimated these costs considering the distance between the two locations (e.g., Conte 2022), this approach potentially minimizes the role of some significant determinants other than transport costs such as family and friends' networks, amenities, culture, language, law and order, and potential discrimination that cannot be restricted to distance measurement (Simpson 2022).

In order to account for these potential determinants, and not rely only on distance, we use migration data from Ceausu et al. (2021). It provides estimates of actual bilateral migration flows between 2005 and 2010 at a very disaggregated level.[7] Our migration costs m_{ik}^{js} are then calibrated by making use of these data together with the inversion of equation (10).[8]

To provide a sense of the migration costs we obtain, we show in Table 2 a regression of our calibrated costs against bilateral distance and real income at destination.

The results emphasize the capacity of our model to adjust the migration costs relative to the distance between locations. In particular, the distance elasticity of the calibrated migration costs is 0.22. This is close to the values found in the literature, as Conte (2022) finds 0.46 while Bryan and Morten (2019) finds 0.15 for Indonesia and 0.02 for the United States.

As shown in Figure A.4 of Appendix C.3, the calibrated migration costs are much higher in magnitude than the literature, indicating that migration barriers may have been underestimated. Here, our approach implicitly accounts for non-monetary components of migration costs, such as language barriers, likely explaining this difference in magnitude.

Local distribution of budget constraint The calibration of the model requires a fit of the distribution of budget constraint $\Phi_i(.)$ in all locations. We assume a lognormal distribution of mean w_i^s and standard deviation v_i^s. The mean w_i^s is pinned down by using local average income from Rossi-Hansberg and Zhang (2025), while v_i^s is calibrated using the local Gini coefficient computed with the wealth index from DHS data.[9]

7. Data are available at the administrative level 1 or 2, depending on countries, and rely on census sources from IPUMS-I.

8. See Appendix C.2 for an extensive description of the model inversion and of our numerical algorithm. Note that to obtain sector-specific migration flows, we use our reconstruction of population in rural and urban areas by exploiting data from the Global Human Settlement project in 2005 and 2010.

9. For the districts where DHS data are not available around year 2010, we use use instead their Gini coefficient in the distribution of the Global Gridded Relative Deprivation Index (CIESIN 2022).

Table 2: Calibrated migration costs validation

Dependent Variable:	Calibrated migration costs (log)				
Model:	(1)	(2)	(3)	(4)	(5)
Distance (log)	0.21***	0.22***	0.03***	0.03***	0.03***
	(0.003)	(0.003)	(0.002)	(0.002)	(0.002)
Dest. real income (log)		0.18***		0.07***	0.07***
		(0.001)		(0.0005)	(0.0005)
Linguistic distance					0.02**
					(0.009)
Fixed-effects					
Origin	Y	Y	Y	Y	Y
Country orig-dest	N	N	Y	Y	Y
Observations	3,246,192	3,246,192	3,246,192	3,246,192	3,243,096
Mean dep. var.	4.0	4.0	4.0	4.0	4.0

Notes: The table reports the estimation of the income elasticity of migration. The distance is computed between the population centers of the districts. Linguistic distance is computed using the LEDA R-package (Muller-Crepon et al. 2022) and the Murdock map (Murdock 1959).

Other key parameters. Finally, we borrow a set of key parameters, such as some elasticities of substitution between crops, from the recent literature in the field. Table 3 summarizes the sources and values of those parameters.

Model validation As our calibration strategy is designed to fit a broad set of key moments, only a limited number of untargeted moments remain. Among these, let us focus on two outcomes of particular interest: GDP and harvested area per district.

The model performs reasonably well on both dimensions, as illustrated by Figure A.2. For local GDP, we obtain a slope of 0.88 and an R-squared of 0.86, indicating that the model captures much of the observed spatial variation in regional income. For the harvested area, we find a slope of 0.67 and an R-squared of 0.57, suggesting a good match between predicted and actual land use patterns across districts.

Table 3: Behavioral parameters taken from the literature

Parameter	Description	Source
$\alpha_A = 0.6$	Crop land share in production	Fajgelbaum and Redding (2022)
$\theta = 1.1$	Dispersion of within-admin land productivity distribution	Gouel and Laborde (2021)
$\nu = 3$	Dispertion of workers distribution preferences for locations	Morten and Oliveira (2024)
$\eta_k = 5.4$	Elasticity of substitution between varieties (agriculture)	Costinot et al. (2016)
$\eta_M = 4$	Elasticity of substitution between varieties (manufacturing)	Desmet et al. (2018)
$\sigma = 0.26$	Elasticity of substitution between goods for final demand	Conte (2022)
$\delta = 0.16$	Distance elasticity of trade costs	Conte (2022)
$\tau = 7.8$	Cross country trade tariffs	Conte (2022)
$\gamma = 2.5$	Elasticity of substitution between agricultural goods	Conte (2022)
$\epsilon_A = 0.2$	Non-homotetic parameter for agricultural goods	Conte (2022)
$\epsilon_M = 1$	Non-homotetic parameter for non-agricultural goods	Conte (2022)

Additionally, in taking into account frictions from the agricultural sector to the non-agricultural sector, we can reproduce a particular feature of the SSA economy: a high share of agricultural employment and a productivity gap between the agricultural and the non-agricultural sector. Figure A.3 provides a country-level fit of these two moments. Our model can predict shares of agricultural employment of 75%.[10]

10. Outliers come from the fact that we estimate agricultural employment based on urbanization, while for some SSA countries, these two variables are not perfectly correlated.

5 Results

This section presents the results of our quantification exercise. We are interested in the share of the labor force trapped by climate change, and we aim to quantify the economic cost of this misallocation for the SSA economy. To this end, we implement the counterfactual analysis in three distinct steps.

First, we simulate the spatial equilibrium of the economy with population projections (at origin) in 2080. This allows us to trace migration and development patterns without climate change until that time horizon.

Second, we add the effect of climate change on land productivity until 2080. To do this, we exploit the FAO-GAEZ data on potential yields under the RCP8.5 scenario for all the crops included in our analysis. The difference between the first and the second step thus allows us to identify the effect of climate change on the SSA economy by 2080. We refer to this result as the *baseline*.

Third, we consider the same differential with future climate conditions but in an economy where the budget constraint is removed. Hence, the difference between the baseline and the third step identifies the impact of liquidity constraints on labor misallocations and (mis-) adaptation.

We start by presenting the results for the whole SSA economy and then focus on spatial heterogeneities.

Aggregate results. Table 4 presents aggregate results for all SSA. The first column depicts the baseline, which is the difference between the cases with and without climate change in 2080. The second column presents the case without the liquidity constraint. In each instance, we show changes in welfare, migration, and immobility.

According to the model, a total of 29M workers will migrate to new locations as a result of climate change in 2080 (column 1). This estimate is close to that of Conte (2022), who estimates total migration at slightly more than 22M workers. Note that our model includes a broader set of crops and accounts for intersectoral wage differentials, which may help refine the magnitude of predicted migration flows.

We now turn to the "net trapped workers", which are those that *would* have migrated but are not as a result of climate change. We find that as many as 31M are trapped by climate change. Put differently, these workers cannot migrate to new sector-region pairs as a result of their climate-induced liquidity constraint.

Table 4: The Economy in 2080 under RCP8.5 relative to no Climate Change

		(1) Baseline	(2) No budget constraint
Climate migration (M)	$\Delta N_i \vert \Delta N_i > 0$	29.56	83.72
Net trapped workers (M)	$\Delta N_{b,i}$	30.70	—
Real income pc change (%)	Δv_i	-4.06	-2.77
Non-ag. emp. change (%)	ΔN_i^M	-0.62	-2.68
Welfare change (%)	ΔW_i	-2.62	-1.84

Notes: The table presents the aggregate results for SSA (Panel A) and by country (Panel B). The *baseline* scenario is the difference between the RCP8.5 and the no climate change scenario in 2080. The *no budget constraint* scenario is the difference between the RCP85 when we remove the budget constraint from equation (10) and the no climate change scenario. The *low mig. costs* presents a case where migration costs are equal to the square root of their value in columns (1) and (2).

On average, net income across districts decreases by 4% as a result of climate change, and manufacturing employment by 0.6%. This result comes from two mechanisms in the model. First, the decline in agricultural yields due to new climate conditions increases labor demand in agriculture to satisfy food requirements, as recently studied by Nath (2025). Second, non-homothetic preferences reinforce this mechanism. As yields decline and income falls, the share of household expenditure devoted to food increases, particularly in the most affected regions (see Figure A.9). This pulls labor into the agricultural sector, thereby hindering structural transformation.

What is the overall cost for the economy? Examining our measure of welfare, which is composed of wages and land rents (in real terms) given migration costs (see equation (25)), we find that it decreases by 2.62% in 2080 as a result of climate change. Part of this substantial decline comes from the inability of labor to relocate across locations and sectors, as we discuss now.

To understand the role played by constraints on financial resources, let us examine column (2), which presents the results in the absence of a budget constraint. We find that the average welfare losses due to climate change fall to 1.84%. This means that, according to our model, liquidity frictions in the presence of climate change cause an additional 0.8 p.p. welfare loss in the SSA economy. Likewise, regarding changes in real income per capita, the additional cost is estimated at around 1.3 p.p. by 2080.

When the budget constraint is removed, the model predicts that 84M workers would migrate in response to climate change. This figure is 2.8 times higher than in the baseline scenario. This is not surprising as it reflects both climate-induced migration and additional migration resulting from the removal of financial constraints.

This first set of results highlights how resource constraints will affect the aggregate costs of future climate conditions in the SSA economy. It inevitably hides important disparities across countries and districts due to differences in the spatial distribution of climate shocks and initial endowments. We now turn to the description of these heterogeneous impacts.

Distributional impacts and immobility across districts in SSA. We start by describing the consequences of the budget constraint on labor misallocation. In Figure 3, we present the number of net trapped workers.

Figure 3: Climate-induced trapped workers

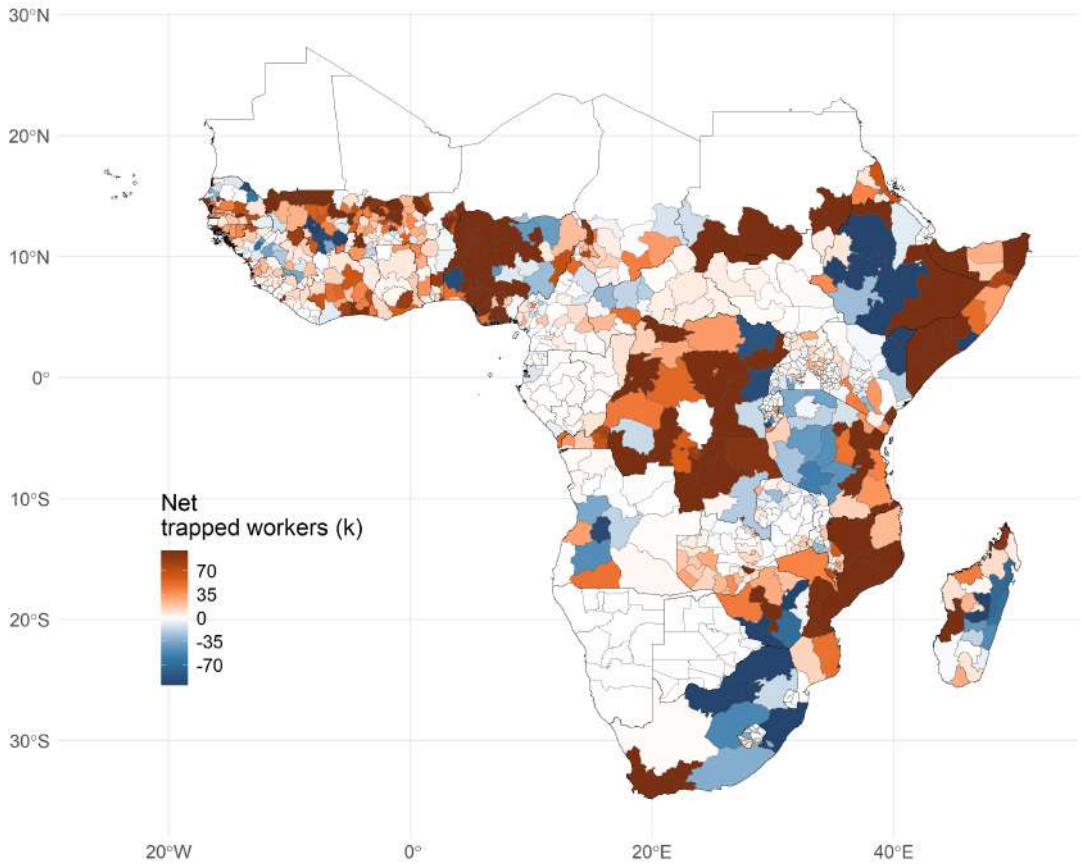

Note: Trapped workers are those who stay in their region-sector pair of origin while they would have moved without the budget constraint. The map shows the absolute difference in trapped workers between the RCP8.5 scenario and the no climate change scenario in 2080 at baseline.

While Table 4 showed that climate change prevented over 30 million workers from relocating, Figure 3 reveals that the impacts vary substantially both between and within countries in SSA. In West Africa, for example, our model predicts that in several districts of Nigeria, Niger, and Mali, more than 70,000 workers will be unable to migrate in response to climate shocks. A similar magnitude of immobility is observed in many districts across East

Africa, including Ethiopia, Somalia, and Sudan. In both the Central African Republic and the Democratic Republic of Congo, the number of climate-constrained workers also exceeds 70,000. Other highly affected areas include Mozambique, parts of Madagascar, and regions of South Africa.

In the latter, the effects are particularly contrasted. In districts located in the eastern part of the country, around Lesotho, climate change is projected to facilitate migration for some workers who would not have been able to under current conditions. This is also true in some parts of Ethiopia and Tanzania.

This pattern in the distribution of trapped workers is naturally correlated with the variation in yields expected by 2080, as shown by Figure A.1. We now turn to an analysis of the economic mechanisms that underlie these spatial disparities in migration constraints and their consequences on welfare and other key indicators.

The role of budget constraint. Having described the patterns of immobility caused by climate change, we now focus on the role played by the budget constraint. In panel (a) of Figure 4, we show how welfare varies across space in the baseline scenario.

Figure 4: The distributional impact of climate change on welfare according to the inclusion of liquidity constraint

(a) Baseline

(b) Baseline vs no budget constraint

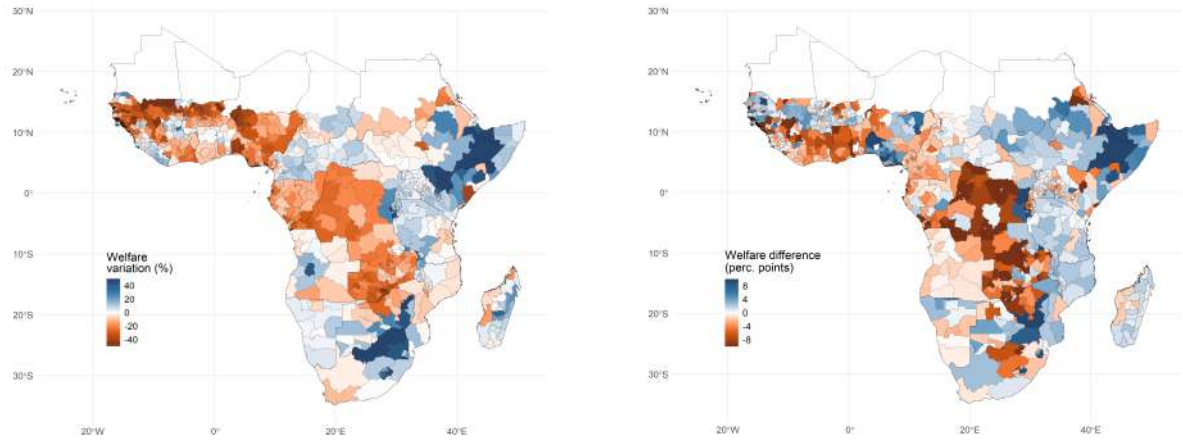

Note: Panel 4a shows the variation in welfare between no climate change and RCP8.5 scenarios, when both scenarios integrate budget constraints. Panel 4b shows the difference, in percentage points, between the variation in welfare with no climate change and RCP8.5 scenarios with budget constraint, and the same variation without budget constraint.

Our model predicts that welfare declines in many parts of SSA, especially where workers are unable to migrate. In Nigeria alone, where the model predicts 13 million trapped workers (see Table A.3), welfare losses reach up to 40 percent in certain districts. These losses are

primarily driven by sharp declines in local wages, particularly in the non-agricultural sector, as illustrated in panel (c) of Figure A.8. There, the combination of high demographic pressure and significant reductions in agricultural yields accounts for the severity of climate-induced immobility in these regions.

Recall that our model does not incorporate sources of growth such as capital accumulation or innovation. All variations in wealth arise only from changes in agricultural yields, given the demographic structure projected for 2080. As a result, in areas affected by climate change where labor supply increases substantially, putting downward pressure on wages, the tightening of the budget constraint becomes particularly salient.

Panel (b) of Figure 4 isolates the role of the budget constraint in shaping spatial patterns of climate adaptation. Positive values (in blue) indicate districts where welfare variation is higher when the budget constraint binds, relative to the counterfactual without it. Conversely, negative values (in orange) correspond to districts where welfare variation is higher in the absence of a binding constraint. In Benin, for example, the budget constraint amplifies the adverse effects of climate change in many districts. While the average predicted welfare loss in the absence of a budget constraint is 1.12% (see Table A.3), this loss exceeds 4% when the liquidity constraint is binding. The latter thus reinforces the negative welfare impacts of climate change in the country.

Releasing the budget constraint would also allow for lowering the burden of climate shocks in many districts of the central part of SSA. There, because labor cannot fully relocate across sector-region pairs, many districts cannot adapt as well as in the absence of liquidity constraints, and this results in either larger losses or lower gains in welfare.

These results highlight the role played by liquidity constraints in the way the SSA economy can adapt to climate change. With a model that would not incorporate that critical feature, one would underestimate the costs of future weather conditions. Overall, we find a 0.8 p.p. difference in the prediction of the rate of change in welfare as a result of climate change with and without budget constraints. For income per capita, there is a 1.2 p.p. difference. Perhaps more importantly, if our analysis did not incorporate budget constraints, our model would predict that the spatial distribution of climate impacts on the economy would be significantly different. Precisely, one would overstate the capacity of some regions to attract workers because migration, a key adaptation tool, would be overestimated.

6 Conclusion

In this paper, we have studied how climate change creates spatial misallocations of labor in SSA and how costly it is in return for economic development. To do this, we first leveraged data on migrations in African districts since 2000 to empirically assess the impact of droughts conditionally on income. Second, we built a quantitative model of migration and trade with spatial frictions, multiple crops, and where workers face liquidity constraints. We then took our model to the data to quantify the effect of climate change in 2080.

In the empirical part, we highlight that poorer workers – proxied by their level of education – exhibit a lower capacity for migration as a response to climate shocks, as measured by droughts. This is not the case for the rest of the income distribution, for whom droughts do cause an increase in the likelihood of leaving one's district. This result holds using different specifications, including long differences. This was our first contribution, providing evidence that inequalities in space create different responses to shocks and that those shocks may block part of the labor force.

Motivated by the empirical findings, we developed a quantitative model to assess the aggregate welfare cost of immobility and to characterize its spatial distribution. The model predicted that climate change would generate substantial welfare losses across nearly all countries in SSA, with approximately 31 million workers unable to migrate by 2080. Liquidity constraints amplify losses, increasing the aggregate welfare cost of climate change by nearly one percentage point. Many workers who would have migrated to adapt to new climatic conditions are prevented from doing so due to negative income shocks in the agricultural sector.

We also showed the crucial distributional impacts of immobility. In countries like the Democratic Republic of Congo, for example, welfare losses predicted by our model exceed 10%. In all, this suggests that not all workers in all locations react the same way to shocks. More broadly, we showed that liquidity constraints are likely to generate significant misallocations of labor, with potentially far-reaching economic and political implications. These results highlight the importance of anticipating and addressing the unequal effects of climate change in order to support the populations most at risk.

References

Bathiany, Sebastian, et al. 2018. "Climate Models Predict Increasing Temperature Variability in Poor Countries." *Science Advances* 4, no. 5 (May): eaar5809. https://doi.org/10.1126/sciadv.aar5809.

Bazzi, Samuel. 2017. "Wealth Heterogeneity and the Income Elasticity of Migration." *American Economic Journal: Applied Economics* 9, no. 2 (April): 219–255. ISSN: 1945-7782. https://doi.org/10.1257/app.20150548.

Berlemann, Michael, and Max Friedrich Steinhardt. 2017. "Climate Change, Natural Disasters, and Migration—a Survey of the Empirical Evidence." *CESifo Economic Studies* 63, no. 4 (December): 353–385. ISSN: 1610-241X. https://doi.org/10.1093/cesifo/ifx019.

Borderon, Marion, et al. 2019. "Migration influenced by environmental change in Africa." *Demographic Research* 41:491–544.

Bozzola, Martina, and Melinda Smale. 2020. "The Welfare Effects of Crop Biodiversity as an Adaptation to Climate Shocks in Kenya." *World Development* 135 (November): 105065. ISSN: 0305-750X. https://doi.org/10.1016/j.worlddev.2020.105065.

Bryan, Gharad, and Melanie Morten. 2019. "The aggregate productivity effects of internal migration: Evidence from Indonesia." *Journal of Political Economy* 127 (5): 2229–2268.

Burzyński, Michał, et al. 2022. "Climate Change, Inequality, and Human Migration." *Journal of the European Economic Association* 20, no. 3 (June): 1145–1197. ISSN: 1542-4766. https://doi.org/10.1093/jeea/jvab054.

Cattaneo, Cristina, and Giovanni Peri. 2016. "The migration response to increasing temperatures." *Journal of development economics* 122:127–146.

Cattaneo, Cristina, et al. 2019. "Human Migration in the Era of Climate Change." *Review of Environmental Economics and Policy* 13, no. 2 (July): 189–206. ISSN: 1750-6816. https://doi.org/10.1093/reep/rez008.

Ceausu, Silvia, et al. 2021. "Mapping gender-disaggregated migration movements at subnational scales in and between low- and middle-income countries," https://doi.org/10.5258/SOTON/WP00673.

Center For International Earth Science Information Network-CIESIN-Columbia University. 2022. *Global Gridded Relative Deprivation Index (GRDI), Version 1.* https://doi.org/10.7927/3XXE-AP97.

Chatterjee, Sumanta, et al. 2022. "Soil Moisture as an Essential Component for Delineating and Forecasting Agricultural Rather than Meteorological Drought." *Remote Sensing of Environment* 269 (February): 112833. ISSN: 0034-4257. https://doi.org/10.1016/j.rse.2021.112833.

Clemens, Michael A, and Mariapia Mendola. 2024. "Migration from developing countries: Selection, income elasticity, and Simpson's paradox." *Journal of Development Economics* 171:103359.

Colmer, Jonathan. 2021. "Temperature, labor reallocation, and industrial production: Evidence from India." *American Economic Journal: Applied Economics* 13 (4): 101–124.

Comin, Diego, et al. 2021. "Structural Change With Long-Run Income and Price Effects" [in en]. Citation Key: Comin2021, *Econometrica* 89 (1): 311–374. ISSN: 1468-0262. https://doi.org/10.3982/ECTA16317.

Conte, Bruno. 2022. "Climate Change and Migration: The Case of Africa." *SSRN Electronic Journal,* ISSN: 1556-5068. https://doi.org/10.2139/ssrn.4226415.

Conte, Bruno, et al. 2021. "Local Sectoral Specialization in a Warming World." *Journal of Economic Geography* 21, no. 4 (July): 493–530. ISSN: 1468-2702. https://doi.org/10.1093/jeg/lbab008.

Costinot, Arnaud, et al. 2016. "Evolving Comparative Advantage and the Impact of Climate Change in Agricultural Markets: Evidence from 1.7 Million Fields around the World." *Journal of Political Economy* 124, no. 1 (February): 205–248. ISSN: 0022-3808. https://doi.org/10.1086/684719.

Cruz, José-Luis, and Esteban Rossi-Hansberg. 2021. *The economic geography of global warming.* Technical report. National Bureau of Economic Research.

Defrance, Dimitri, et al. 2022. "Migration response to drought in Mali. An analysis using panel data on Malian localities over the 1987-2009 period" [in en]. Citation Key: Defrance2022, *Environment and Development Economics* (August): 1–20. ISSN: 1355-770X, 1469-4395. https://doi.org/10.1017/S1355770X22000183.

Dell, Melissa, et al. 2014. "What Do We Learn from the Weather? The New Climate-Economy Literature." *Journal of Economic Literature* 52, no. 3 (September): 740–798. ISSN: 0022-0515. https://doi.org/10.1257/jel.52.3.740.

Desmet, Klaus, and Esteban Rossi-Hansberg. 2023. "Climate Change Economics over Time and Space."

Desmet, Klaus, et al. 2018. "The Geography of Development." *Journal of Political Economy* 126 (3): 903–983. https://doi.org/10.1086/697084. eprint: https://doi.org/10.1086/697084.

Di Falco, Salvatore, et al. 2024. "Leaving Home: Cumulative Climate Shocks and Migration in Sub-Saharan Africa" [in en]. Keywords: cumul_shocks_mig, *Environmental and Resource Economics* 87, no. 1 (January): 321–345. ISSN: 1573-1502. https://doi.org/10.1007/s10640-023-00826-x.

Fajgelbaum, Pablo, and Stephen J. Redding. 2022. "Trade, Structural Transformation, and Development: Evidence from Argentina 1869–1914." *Journal of Political Economy* 130, no. 5 (May): 1249–1318. ISSN: 0022-3808, 1537-534X. https://doi.org/10.1086/718915.

Gazeaud, Jules, et al. 2023. "Cash transfers and migration: Theory and evidence from a randomized controlled trial." *Review of Economics and Statistics* 105 (1): 143–157.

Gollin, Douglas, et al. 2013. "The agricultural productivity gap." *The Quarterly Journal of Economics* 129 (2): 939–993.

Gouel, Christophe, and David Laborde. 2021. "The Crucial Role of Domestic and International Market-Mediated Adaptation to Climate Change." *Journal of Environmental Economics and Management* 106 (March): 102408. ISSN: 0095-0696. https://doi.org/10.1016/j.jeem.2020.102408.

Grogger, Jeffrey, and Gordon H. Hanson. 2011. "Income Maximization and the Selection and Sorting of International Migrants." *Journal of Development Economics,* Symposium on Globalization and Brain Drain, 95, no. 1 (May 1, 2011): 42–57. ISSN: 0304-3878. https://doi.org/10.1016/j.jdeveco.2010.06.003.

Henderson, J Vernon, et al. 2017. "Has climate change driven urbanization in Africa?" *Journal of development economics* 124:60–82.

Hoffmann, Roman, et al. 2024. "Drought and aridity influence internal migration worldwide." *Nature Climate Change,* 1–9.

Kubik, Zaneta, and Mathilde Maurel. 2016. "Weather Shocks, Agricultural Production and Migration: Evidence from Tanzania." *The Journal of Development Studies* 52, no. 5 (May): 665–680. ISSN: 0022-0388, 1743-9140. https://doi.org/10.1080/00220388.2015.1107049.

Liu, Yaling, et al. 2015. "Agriculture Intensifies Soil Moisture Decline in Northern China." *Scientific Reports* 5, no. 1 (July): 11261. ISSN: 2045-2322. https://doi.org/10.1038/srep11261.

Marchal, Léa, and Claire Naiditch. 2020. "How Borrowing Constraints Hinder Migration: Theoretical Insights from a Random Utility Maximization Model" [in en]. Citation Key: Marchal2020, *The Scandinavian Journal of Economics* 122 (2): 732–761. ISSN: 1467-9442. https://doi.org/10.1111/sjoe.12355.

McCarthy, Nancy, et al. 2021. "Droughts and Floods in Malawi: Impacts on Crop Production and the Performance of Sustainable Land Management Practices under Weather Extremes." *Environment and Development Economics* 26, nos. 5-6 (October): 432–449. ISSN: 1355-770X, 1469-4395. https://doi.org/10.1017/S1355770X20000455.

Meyer, Jessica. 2023. "How Do Forests Contribute to Food Security Following a Weather Shock? Evidence from Malawi." *World Development* 169 (September): 106307. ISSN: 0305-750X. https://doi.org/10.1016/j.worlddev.2023.106307.

Millán, Teresa Molina, et al. 2020. "Experimental long-term effects of early-childhood and school-age exposure to a conditional cash transfer program." *Journal of Development Economics* 143:102385.

Morten, Melanie, and Jaqueline Oliveira. 2024. "The Effects of Roads on Trade and Migration: Evidence from a Planned Capital City" [in en]. Keywords: roads$_m$ig$_c$osts, *American Economic Journal: Applied Economics* 16, no. 2 (April): 389–421. ISSN: 1945-7782, 1945-7790. https://doi.org/10.1257/app.20180487.

Muller-Crepon, Carl, et al. 2022. "Linking Ethnic Data from Africa (LEDA)" [in en]. Citation Key: MullerCrepon2022, *Journal of Peace Research* 59, no. 3 (May): 425–435. ISSN: 0022-3433. https://doi.org/10.1177/00223433211016528.

Murdock, George Peter. 1959. *Africa: Its Peoples and Their Culture History* [in en]. Google-Books-ID: Wt5xAAAAMAAJ. McGraw-Hill.

Nath, Ishan. 2025. "Climate change, the food problem, and the challenge of adaptation through sectoral reallocation." *Journal of Political Economy* 133 (6): 000–000.

Peri, Giovanni, and Akira Sasahara. 2019. *The Impact of Global Warming on Rural-Urban Migrations: Evidence from Global Big Data.* Technical report w25728. Cambridge, MA: National Bureau of Economic Research, April. https://doi.org/10.3386/w25728.

Pignède, Edouard. 2025. "Who carry the burden of climate change? Heterogeneous impacts of droughts in Sub-Saharan Africa." *American Journal of Agricultural Economics.*

Ranasinghe, Roshanka, et al. 2021. "Climate Change Information for Regional Impact and for Risk Assessment." In *Climate Change 2021: The Physical Science Basis. Contribution of Working Group I to the Sixth Assessment Report of the Intergovernmental Panel on Climate Change [Masson-Delmotte, V., P. Zhai, A. Pirani, S. L. Connors, C. Péan, S. Berger, N. Caud, Y. Chen, L. Goldfarb, M. I. Gomis, M. Huang, K. Leitzell, E. Lonnoy, J. B. R. Matthews, T. K. Maycock, T. Waterfield, O. Yelekçi, R. Yu and B. Zhou (Eds.)]* Cambridge University Press, 1767–1926. In Press. Cambridge, United Kingdom and New York, NY, USA: Cambridge University Press.

Redding, Stephen J., and Esteban Rossi-Hansberg. 2017. "Quantitative Spatial Economics." *Annual Review of Economics* 9, no. 1 (August): 21–58. ISSN: 1941-1383, 1941-1391. https://doi.org/10.1146/annurev-economics-063016-103713.

Rigaud, Kanta Kumari, et al. 2018. *Groundswell: Preparing for Internal Climate Migration* [in en]. Publisher: World Bank, Washington, DC Citation Key: Rigaud2018. Washington, DC, March.

Rossi-Hansberg, Esteban, and Jialing Zhang. 2025. *Local GDP estimates around the world.* Keywords: gridded$_g dp$, January.

Schiavina, Marcello, Sergio Freire, et al. 2023. *GHS-POP R2023A - GHS population grid multitemporal (1975-2030)* [in en]. https://doi.org/10.2905/2FF68A52-5B5B-4A22-8F40-C41DA8332CFE.

Schiavina, Marcello, Michele Melchiorri, et al. 2023. *GHS-SMOD R2023A - GHS settlement layers, application of the Degree of Urbanisation methodology (stage I) to GHS-POP R2023A and GHS-BUILT-S R2023A, multitemporal (1975-2030)* [in en]. https://doi.org/10.2905/A0DF7A6F-49DE-46EA-9BDE-563437A6E2BA.

Simpson, Nicole B. 2022. "Demographic and economic determinants of migration." *IZA World of Labor,* https://doi.org/10.15185/izawol.373.v2.

Tombe, Trevor, and Xiaodong Zhu. 2019. "Trade, Migration, and Productivity: A Quantitative Analysis of China." *American Economic Review* 109, no. 5 (May): 1843–1872. ISSN: 0002-8282. https://doi.org/10.1257/aer.20150811.

United Nations. 2022. *World Population Prospects 2022: Summary of Results.* Statistical Papers - United Nations (Ser. A), Population and Vital Statistics Report. United Nations, Department of Economic and Social Affairs, Population Division, August. ISBN: 978-92-1-001438-0. https://doi.org/10.18356/9789210014380.

Vicente-Serrano, Sergio M., et al. 2010. "A Multiscalar Drought Index Sensitive to Global Warming: The Standardized Precipitation Evapotranspiration Index." *Journal of Climate* 23, no. 7 (April): 1696–1718. ISSN: 0894-8755, 1520-0442. https://doi.org/10.1175/2009JCLI2909.1.

Zappalà, Guglielmo. 2023. "Drought Exposure and Accuracy: Motivated Reasoning in Climate Change Beliefs." *Environmental and Resource Economics* 85, no. 3 (August): 649–672. ISSN: 1573-1502. https://doi.org/10.1007/s10640-023-00779-1.

Zhou, Zhiling, et al. 2023. "Projecting Global Drought Risk Under Various SSP-RCP Scenarios." *Earth's Future* 11 (5): e2022EF003420. ISSN: 2328-4277. https://doi.org/10.1029/2022EF003420.

Online Appendix

A Appendix tables and figures

A.1 Figures

Figure A.1: Weigthed average changes in crop yields by 2080.

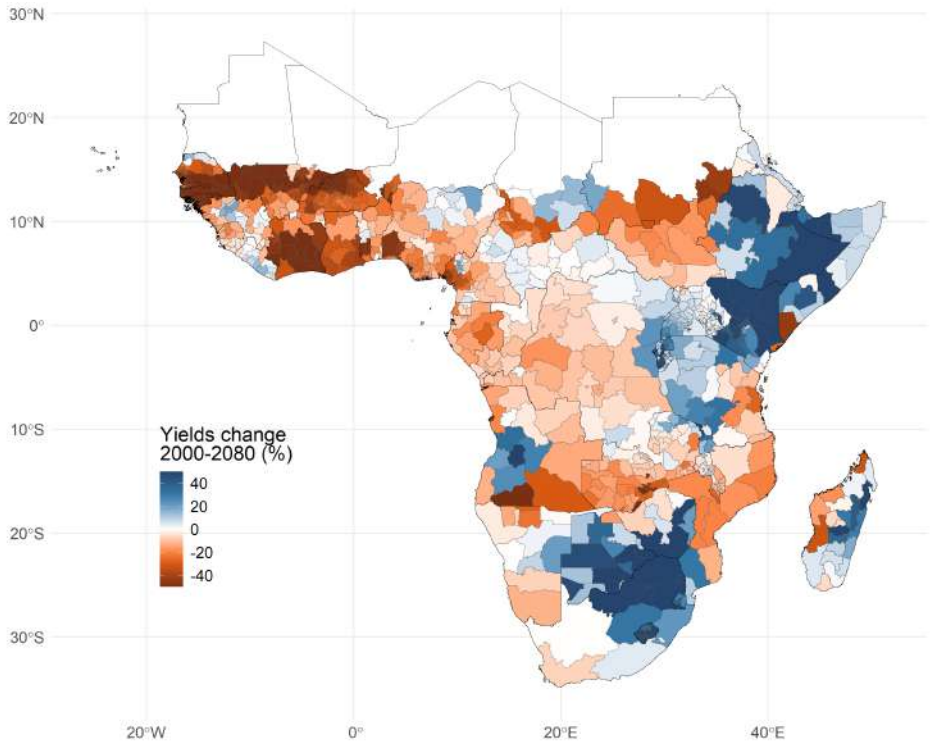

Note: This is the change in the average value of A_i^k weighted by total production value in 2010 for the ten crops of our study between 1980-2010 and 2071-2100, RCP8.5 scenario. Source: GAEZ v4 data.

Figure A.2: Model fit between the initial equilibrium of the model and data.

(a) Local GDP (b) Harvested area

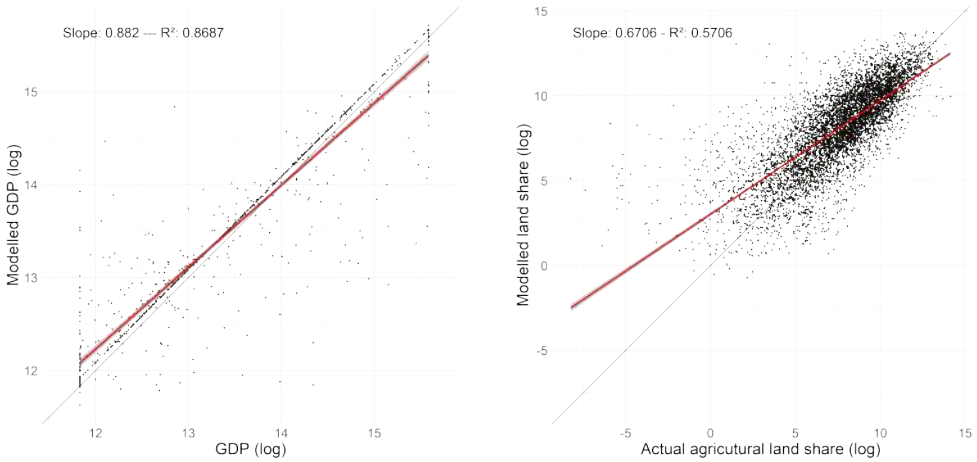

Note: Data on local GDP comes from Rossi-Hansberg and Zhang (2025) and data on harvested area comes from the GAEZ project.

Figure A.3: Model fit between the initial equilibrium of the model and data.

(a) Agricultural employment (b) Agr. productivity gap

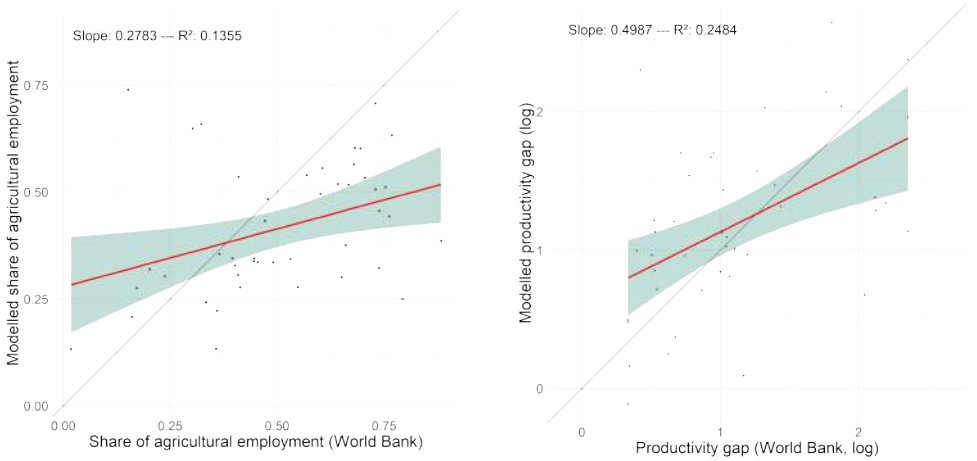

Note: Data on country agricultural employment and country GDP are from the World Bank.

Figure A.4: Comparison of internal migration costs with the literature

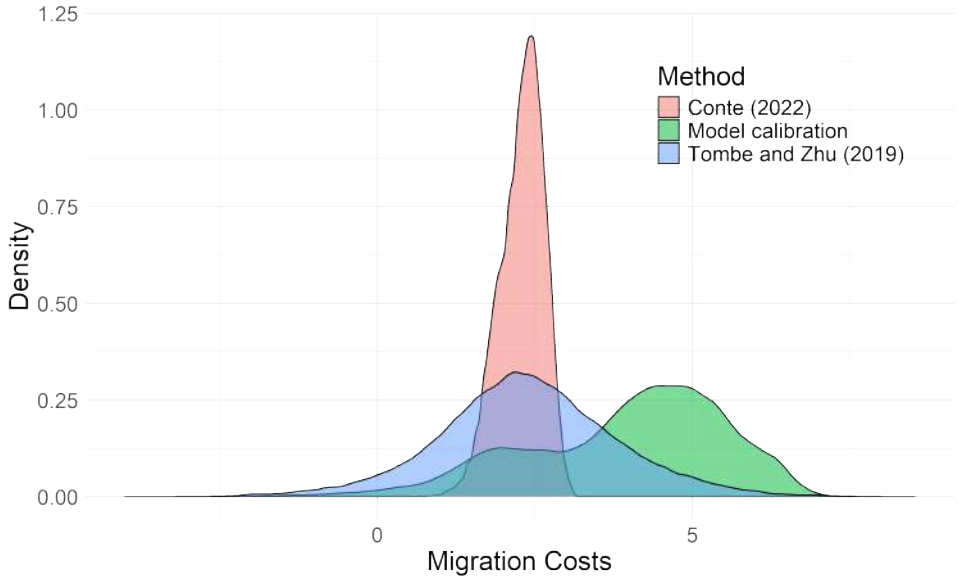

Note: Details on the computation of internal migration costs from Conte (2022) and Tombe and Zhu (2019) are available in Appendix C.3.

Figure A.5: Country distribution of climate change impact

(a) Net migration

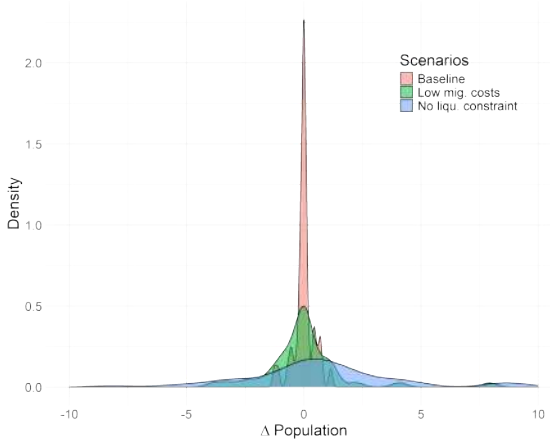

(b) Share of non-agri employment

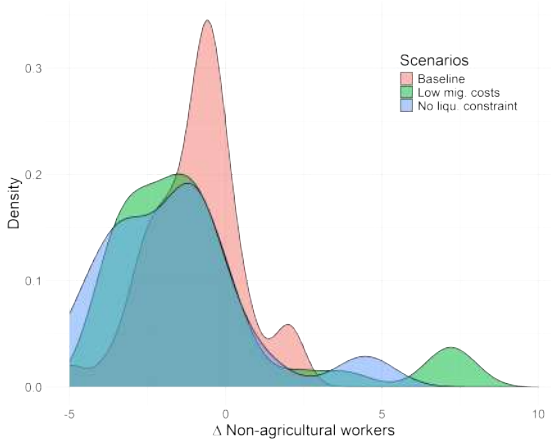

Figure A.6: Country distribution of climate change impact

(a) Welfare

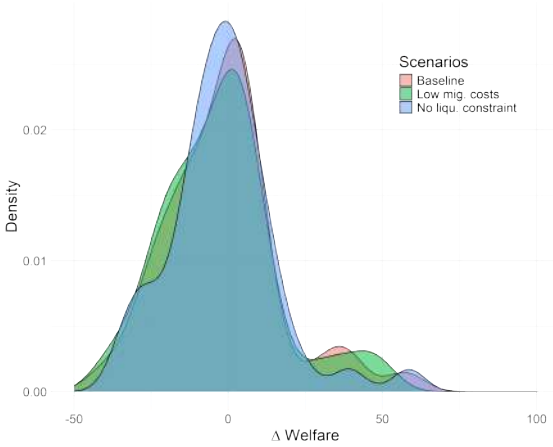

(b) Mean real wage

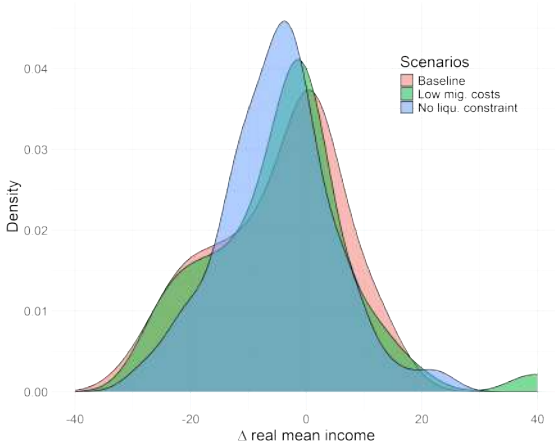

Figure A.7: Predicted variations in population by 2080 under climate change

(a) With budget constraint

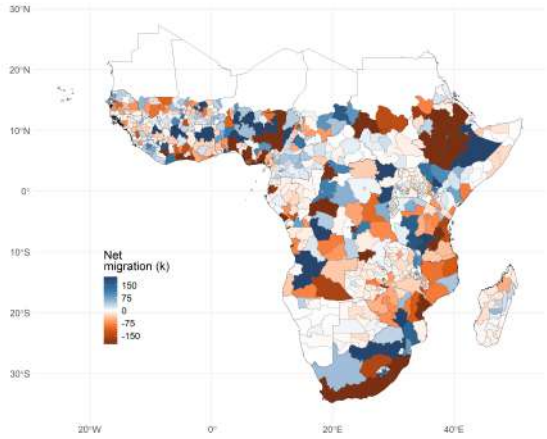

(b) Without budget constraint

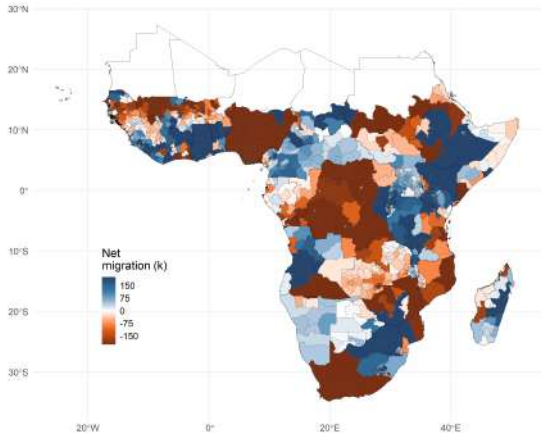

Figure A.8: Predicted variations in wages by 2080 under climate change

(a) Agri. — With budget constraint

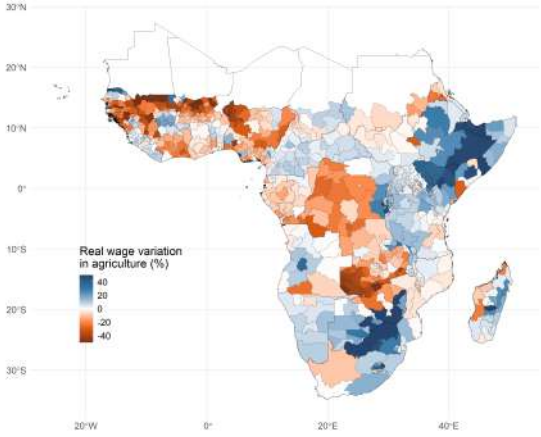

(b) Agri. — Without budget constraint

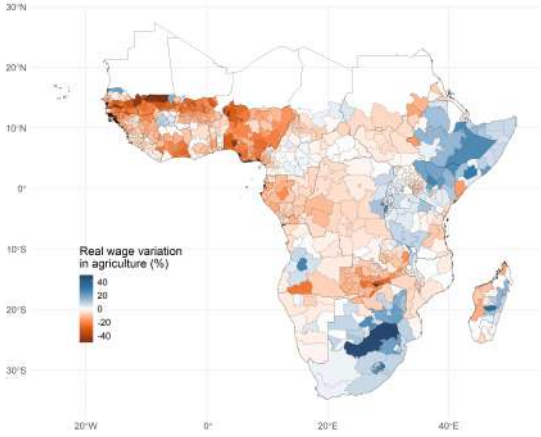

(c) Manuf. — With budget constraint

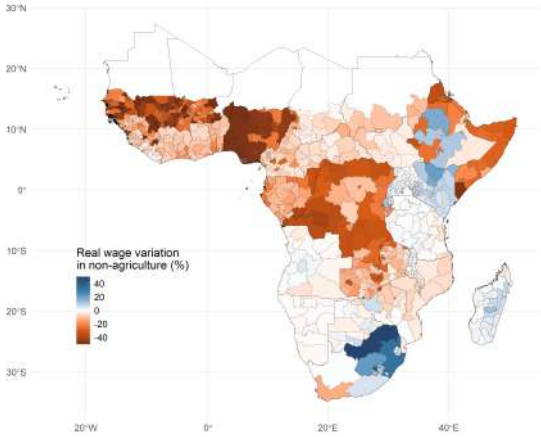

(d) Manuf. — Without budget constraint

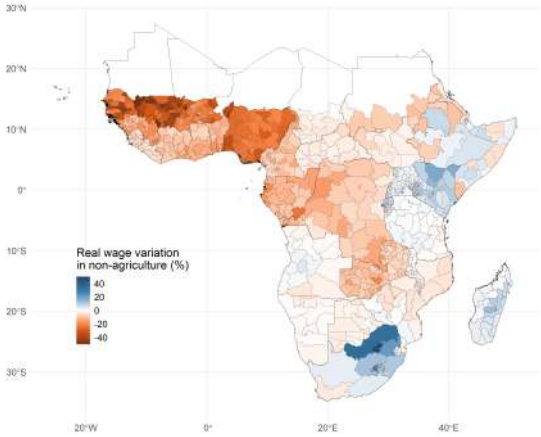

Figure A.9: Predicted variations in agricultural consumption by 2080 under climate change

(a) Agri. — With budget constraint

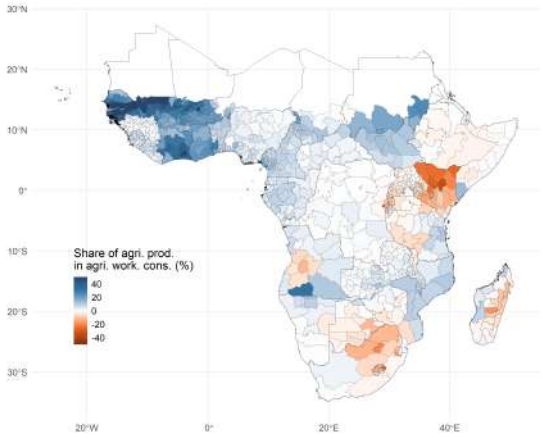

(b) Agri. — Without budget constraint

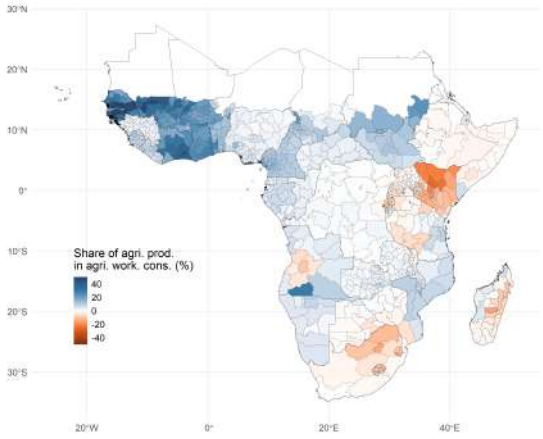

(c) Manuf. — With budget constraint

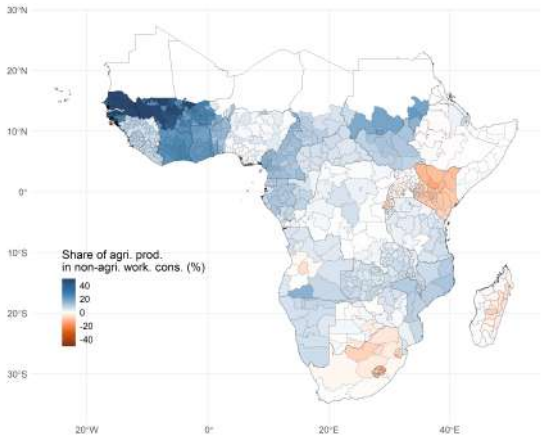

(d) Manuf. — Without budget constraint

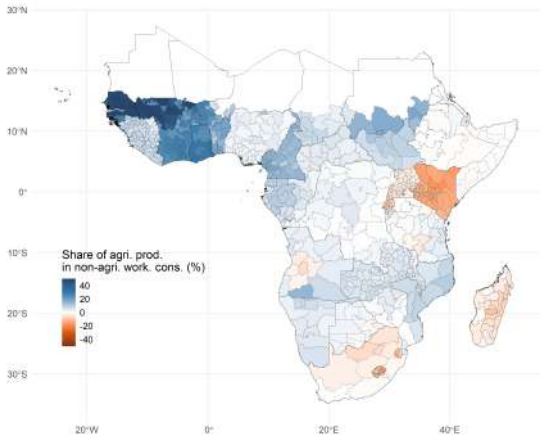

A.2 Tables

Table A.1: Welfare in 2080 under RCP8.5 and no climate change scenario

	(1) No climate change	(2) With climate change	(3) Climate change impact (%)
Panel A - Welfare (W_i)			
Baseline	1.00	0.97	-2.62
No budget constraint	1.17	1.15	-1.84
Low trade costs	1.55	1.48	-4.50
No budg. cons. + Low tra. costs	1.68	1.63	-3.44
Low migration costs	1.17	1.13	-2.96
No budg. cons. + Low mig. costs	1.49	1.46	-2.10
Panel B - Real income per capita (v_i/P_i)			
Baseline	1.00	0.96	-4.06
No budget constraint	1.20	1.17	-2.77
Low trade costs	1.60	1.51	-5.88
No budg. cons. + Low tra. costs	1.75	1.67	-4.62
Low migration costs	1.08	1.04	-4.23
No budg. cons. + Low mig. costs	1.44	1.40	-3.02

Notes: The table presents the aggregate welfare (Panel A) and real income per capita (Panel B) normalized by the baseline total welfare (or real income per capita) in several scenarios, with RCP85 climate change and without climate change. The last column is the impact of climate change in percentage.

Table A.2: The Economy in 2080 under RCP8.5 relative to no Climate Change with alternative specifications

		(1) Baseline	(2) No budget constraint
Panel A - Low trade costs			
Climate migration (M)	$\Delta N_i \vert \Delta N_i > 0$	26.40	52.65
Net trapped workers (M)	$\Delta N_{b,i}$	8.03	—
Real income pc change (%)	Δv_i	-5.88	-4.62
Non-ag. emp. change (%)	ΔN_i^M	-1.67	-2.99
Welfare change (%)	ΔW_i	-4.50	-3.44
Panel B - Homothetic preferences			
Climate migration (M)	$\Delta N_i \vert \Delta N_i > 0$	17.14	24.83
Net trapped workers (M)	$\Delta N_{b,i}$	-1.82	—
Real income pc change (%)	Δv_i	-1.94	-2.04
Non-ag. emp. change (%)	ΔN_i^M	-0.59	-0.62
Welfare change (%)	ΔW_i	-0.43	-0.52

Notes: The table presents the aggregate results for SSA when we consider low trade costs ($\tau_{LTC} = 2.6$) (Panel A) and Homothetic preferences (Panel B). The *baseline* scenario is the difference between the RCP8.5 and the no climate change scenario in 2080. The *no budget constraint* scenario is the difference between the RCP85 when we remove the budget constraint from equation (10) and the no climate change scenario.

Table A.3: Results by country in 2080 under RCP8.5 relative to no Climate Change

	Welfare change (%)		Net migration (M)		Net trap. work.	
	Baseline	No BC	Baseline	No BC	M	% of pop.
Central Africa						
Angola	5.75	5.76	1.14	4.94	-0.06	-0.06
Burundi	37.81	23.74	0.00	1.44	-0.23	-0.66
Central African Republic	2.38	2.45	0.10	0.78	0.04	0.26
Cameroon	-6.48	-4.24	0.04	4.23	0.37	0.49
Congo - Kinshasa	-11.02	-9.74	-0.36	-8.21	4.78	1.68
Congo - Brazzaville	-19.85	-16.73	-0.55	-1.14	0.02	0.10
Gabon	-15.27	-13.31	-0.23	-0.08	-0.01	-0.11
Equatorial Guinea	-14.05	-10.02	0.00	0.09	0.00	-0.02
Rwanda	12.22	16.95	0.18	3.54	-0.01	-0.04
São Tomé & Príncipe	5.16	-5.23	0.00	0.01	0.01	2.59
Chad	-0.45	-0.19	0.07	1.31	0.16	0.35
East Africa						
Djibouti	0.26	-6.20	0.00	-0.07	0.02	0.87
Eritrea	-14.20	-9.01	-0.01	-0.18	0.07	0.94
Ethiopia	14.00	12.32	-0.07	2.16	0.17	0.19
Kenya	11.35	12.49	0.67	8.36	-0.33	-0.30
Madagascar	7.13	6.62	-0.02	1.90	-0.22	-0.31
Mozambique	-2.73	-4.22	-0.69	-1.95	0.79	0.99
Malawi	2.75	1.05	0.12	0.48	0.32	0.60
Sudan	-8.52	-12.01	-0.53	-3.13	0.74	1.73
Somalia	6.40	5.49	-0.18	-0.21	2.92	5.13
South Sudan	-1.39	-3.22	0.05	-0.27	0.01	0.06
Tanzania	3.97	2.79	0.02	1.82	0.53	0.31
Uganda	3.42	3.80	-0.13	4.16	0.15	0.12
Southern Africa						
Botswana	6.05	5.25	-0.05	0.28	0.00	-0.08
Lesotho	38.14	39.16	0.68	1.32	-0.03	-1.11
Namibia	-1.19	-2.25	0.00	0.13	0.00	0.00
Eswatini	28.64	14.35	0.46	0.56	0.00	-0.06
South Africa	57.25	58.62	0.39	9.24	-1.43	-2.11
Zambia	-22.39	-17.72	-1.11	-3.21	0.55	0.98
Zimbabwe	7.10	5.56	-0.02	0.56	-0.50	-1.48
West Africa						
Benin	-4.01	-1.12	0.41	3.59	0.23	0.58
Burkina Faso	-21.65	-20.41	0.75	-2.80	1.87	3.30
Côte d'Ivoire	-15.30	-11.17	-1.27	1.49	0.95	1.38
Cape Verde	2.55	12.50	0.01	0.70	0.00	0.03
Ghana	-7.70	-2.41	0.03	8.44	0.28	0.43
Guinea	-13.21	-11.16	0.11	-1.22	0.17	0.54
Gambia	-54.67	-53.11	-0.05	-1.20	0.42	6.71
Guinea-Bissau	-31.38	-32.23	-0.04	-0.89	0.23	5.19
Liberia	5.60	8.34	0.53	2.49	0.16	1.36
Mali	-27.60	-28.58	0.11	-4.46	1.64	2.47
Niger	-40.32	-35.03	-0.12	-3.48	0.92	3.12
Nigeria	-22.58	-26.25	-0.15	-29.44	12.92	3.27
Senegal	-26.16	-26.73	-0.16	-5.65	1.78	3.47
Sierra Leone	-0.28	0.97	-0.15	1.39	0.21	1.23
Togo	-9.08	-5.64	-0.01	2.19	0.11	0.47

Notes: The table presents the aggregate results by countries of SSA. The *baseline* scenario is the difference between the RCP8.5 and the no climate change scenario in 2080. The *No BC* scenario is the difference between the RCP85 and the no climate change scenario when we remove the budget constraint from equation (10). The first two columns present the welfare change in percentage, the next two columns the net number of migrations in million, and the last two columns the number of trapped workers (for the baseline scenario) in million people and in percentage of the initial population in 2080.

B Estimations

This section describes the data and provides additional results to the empirical models presented in section 2.

B.1 Data

B.1.1 Census data

To compute the migration rate, we use census data from IPUMS-I. These data are representative samples of census data organized by national statistics agencies. They contain data on 10% of the country's population for most censuses (it can go from 2% to 16%). To compute the bilateral migration rate between administrative regions, we follow the procedure of Hoffmann et al. (2024). We use a question on the administrative region of residence a year ago, 5 years ago, 10 years ago, or the previous administrative region of residence. In this latter case, we transform it into a 1-year-ago administrative region of residence. Figure B.1 presents the different countries and the census years used in the study that contain data on migration.

We compute the annual migration rate using the following equation:

$$M_{ijt} = \frac{F_{ijt}}{P_{i[t-I_{it}]} \times I_{it}} \tag{B.1}$$

With F_{ijt}, the number of individuals living in the region i one, five, or ten years ago, and living in the region j at the year t of the census. $P_{i[t-I_{it}]}$ is the total population of the region of origin (sum of people in i that do not move and those who were living in i one, five, or ten years ago). Migration rates by education level are obtained using the same formula when considering only individuals with a particular level of education. Education levels are those defined by the International Standard Classification of Education (ISCED).

B.1.2 Weather and climate data

Climate change strongly modifies temperature and precipitation patterns across the globe, and Sub-Saharan Africa is one of the most impacted locations (Bathiany et al. 2018). One of these impacts is to increase the frequency and intensity of extreme weather events, such as agricultural droughts. Agricultural drought is a shortage of soil moisture that affects crop growth, reducing crop yields (Chatterjee et al. 2022), and, as a result, is a negative shock on the agricultural income of farmers (Pignède 2025). These extreme weather events

Figure B.1: Countries and census years considered from IPUMS

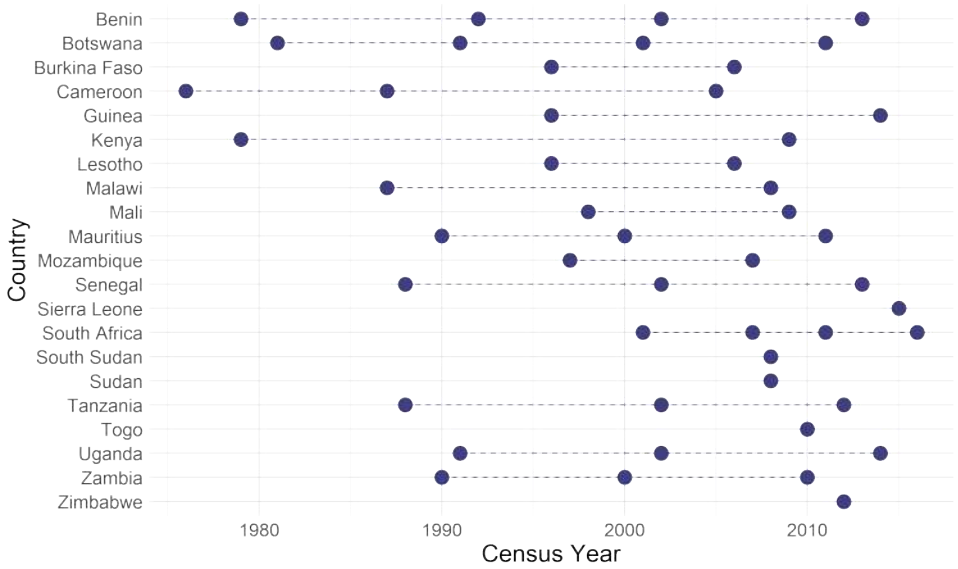

Note: List of countries and census years that contain migration data in Sub-Saharan Africa

are particularly interesting in the study of climate migration as they can push farmers to move because of poor expectations of future revenues. On the other hand, by reducing farmers' income, they can also limit their ability to bear the cost required to migrate.

The literature employs various measures of agricultural drought to examine the impact of weather on agricultural production. These measures are based on meteorological data (e.g., the Standardized Precipitation Index), soil moisture data (e.g., the Soil Moisture Anomaly Index), vegetation cover (e.g., the Normalized Difference Vegetation Index), or a combination of these sources.

This study utilizes the Standardized Precipitation and Evapotranspiration Index (SPEI), which assesses deviations in the climate water balance calculated as the difference between precipitation and potential evaporation relative to long-term averages (Vicente-Serrano et al. 2010). SPEI is regionally comparable and incorporates the temperature component of drought through potential evaporation, enabling improved monitoring of soil moisture compared to indices based solely on precipitation anomalies. Furthermore, because SPEI relies exclusively on meteorological data, it remains independent of local agricultural practices related to vegetation and soil moisture (Liu et al. 2015). This index is also widely adopted in socio-economic studies analyzing the impacts of agricultural drought in sub-Saharan Africa (Kubik and Maurel 2016; Bozzola and Smale 2020; McCarthy et al. 2021; Defrance et al. 2022; Zappalà 2023; Meyer 2023). We compute the SPEI using data on precipitation and potential evaporation from the Climatic Research Unit (CRU) of the University of East Anglia (CRU

Table B.1: Elasticity of migration in response to drought with different drought measures

Dependent Variable:	Migration rate (log)			
Education	Less than primary	Primary	Secondary	Tertiary
Model:	(1)	(2)	(3)	(4)
Droughts	-0.008	0.014	0.036**	0.068*
	(0.016)	(0.013)	(0.016)	(0.035)
Droughts (1-month SPEI)	-0.017	0.005	0.010	0.038
	(0.013)	(0.012)	(0.013)	(0.031)
Droughts (SPEI < -1.5)	0.013	0.018	0.020	0.043
	(0.016)	(0.013)	(0.014)	(0.030)
Droughts (SPEI < -2)	0.033	0.023	0.025	0.048
	(0.025)	(0.019)	(0.017)	(0.038)
Droughts (Use data only from 1950)	0.011	0.021	0.029**	0.039
	(0.016)	(0.013)	(0.015)	(0.033)
Droughts (sum of months with SPEI < -1)	-0.0006	0.002	0.007**	0.014**
	(0.004)	(0.003)	(0.003)	(0.006)
Observations	11,630	11,253	9,773	6,617
Mean dep. var.	0.004	0.006	0.010	0.015

Notes: Results of regression of equation 2 using Poisson maximum likelyhood estimator. Origin-destination and destination-year fixed effects are included in all regressions. The first line presents the baseline (figure 1). The other lines represents the results of the same regression with alternative measures of drought: (i) considering the 1-month SPEI, which will be more representative of meteorological drought than agricultural drought, (ii) considering severe droughts (SPEI < -1.5) and (iii) very severe droughts (SPEI < -2), (iv) using only climate data from 1950 to compute the SPEI (given the increase in mean temperature, it lowers the number of droughts), and (v) summing the number of months with the SPEI inferior to -1 dring the year, which will take into account the duration of the drought.

TS, v.4.08), taking the period 1901-2023 as a reference and using the SPEI R package. The CRU TS dataset is a global climate dataset at 0.5°resolution. It provides monthly climate data from 1901 to 2023, including indicators such as temperature, precipitation, and potential evapotranspiration (PET). These measures are derived from interpolations of climate anomalies using angular-distance weighting based on data from a vast network of weather stations worldwide.

As in Zhou et al. (2023), we consider that agricultural drought impacts a pixel in a year t if the 6-month SPEI falls below -1 (equivalent to one standard deviation below the long-term mean). We then consider the share of each district impacted by drought each year to aggregate it at the district level.

B.2 Additional results

In this section, we propose some additional results to the empirical part presented in section 2.

Table B.2: Elasticity of migration in response to drought according to different distance cut-offs

Dependent Variable:	Migration rate (log)			
Education	Less than primary	Primary	Secondary	Tertiary
Model:	(1)	(2)	(3)	(4)
Panel A: Distance > 1st quartile				
Droughts	0.002	0.019	0.039**	0.065*
	(0.016)	(0.013)	(0.016)	(0.036)
Droughts × Distance > 150 km	-0.354***	-0.245***	-0.155*	0.147
	(0.103)	(0.074)	(0.085)	(0.234)
Panel B: Distance > median				
Droughts	0.004	0.020	0.042**	0.066*
	(0.017)	(0.013)	(0.017)	(0.036)
Droughts × Distance > 300 km	-0.223***	-0.144**	-0.173**	0.051
	(0.072)	(0.066)	(0.086)	(0.169)
Panel C: Distance > 3rd quartile				
Droughts	-0.006	0.015	0.042**	0.069*
	(0.017)	(0.013)	(0.016)	(0.037)
Droughts × Distance > 450 km	-0.029	-0.031	-0.128	-0.016
	(0.079)	(0.069)	(0.093)	(0.192)
Observations	11,630	11,253	9,773	6,617
Mean dep. var.	0.004	0.006	0.010	0.015
Mean mig dist.	204.0	225.1	258.5	279.6

Notes: Results of regression of equation 2 using Poisson maximum likelyhood estimator. Origin-destination and destination-year fixed effects are included in all regressions.

Other measures of drought Table B.1 presents the result of the baseline (figure 1) when we modify the definition of drought. In particular, we consider four alternative measures of drought: (i) considering the 1-month SPEI, which will be more representative of meteorological drought than agricultural drought, (ii) considering severe droughts (SPEI $<$ -1.5) and (iii) very severe droughts (SPEI $<$ -2), (iv) using only climate data from 1950 to compute the SPEI (given the increase in mean temperature, it lowers the number of droughts), and (v) summing the number of months with the SPEI inferior to -1 dring the year, which will take into account the duration of the drought. Overall, results show similar patterns to the baseline (line 1), but with results more imprecise in some specifications. In particular, considering more severe droughts notably reduces the heterogeneity in responses to drought according to education level. In that case, low-educated households also seem to out-migrate in response to droughts (the result being not significantly different from 0). This observation may take root in the concept of "survival migration", defined as temporary moves over short distances (Cattaneo et al. 2019). This type of migration is not the topic of our paper, as our model aimed at studying the long-term migration induced by slow-onset events.

Alternative distance of migration cut-offs Table B.2 shows the results of the migration elasticity response according to the distance of migration (Table 1) with different cut-off distances. Results are really similar if we take a cut-off of 150 kilometers (Panel A), which corresponds to the 1st quartile of distance between districts in the data. When we take a cut-off of 450 kilometers (Panel C), the results are not significantly different from 0. As the mean distance of migration in the data is between 200 and 300 kilometers, the low probability of migration up to 450 kilometers may explain this result.

C Model derivations

C.1 Spatial equilibrium

The spatial equilibrium is a vector of value of production, rent, wages, population distribution and land distribution $\{X_i^k, r_i^k, w_i^s, N_i^s, \pi_i^k\}$ in each region i and sector k given the parameters $\{\eta_k, \alpha_k, \theta, \nu, m_{ik}^{js}, A_i^k, \sigma, \gamma, \epsilon_k, z_i^k, \phi_i, \kappa_{ij}, \Phi_i(.)\}$ that verifies the following set of equations:

$$X_i^k = \sum_{j \in \mathcal{L}} \left(\frac{(r_i^k)^{\alpha_k} (w_i^A)^{1-\alpha_k} \kappa_{ij}}{z_i^k c_k P_j^k} \right)^{1-\eta_k} (P_j^k / P_j^A)^{1-\gamma} \left(\mu_{jA}^A E_j^A N_j^A + \mu_{jM}^A E_j^M N_j^M \right) \tag{C.1}$$

$$X_i^M = \sum_{j \in \mathcal{L}} \left(\frac{w_i^M \kappa_{ij}}{z_i^M P_j^M} \right)^{1-\eta_M} \left(\mu_{jA}^M E_j^A N_j^A + \mu_{jM}^M E_j^M N_j^M \right) \tag{C.2}$$

$$P_{js} = \left(\sum_{k \in \{A,M\}} \left(\Omega_k (P_j^k)^{1-\sigma} \right)^{(1-\sigma)/\epsilon_k} \left(\mu_{js}^k (E_j^s)^{1-\sigma} \right)^{\frac{\epsilon_k - (1-\sigma)}{\epsilon_k}} \right)^{\frac{1}{1-\sigma}} \tag{C.3}$$

$$\mu_{js}^k = \Omega_k \left(\frac{P_j^k}{P_{js}} \right)^{1-\sigma} \left(\frac{E_j^s}{P_{js}} \right)^{\epsilon_k - (1-\sigma)} \tag{C.4}$$

$$P_j^A = \left(\sum_{k \in \mathcal{K}} (P_j^k)^{1-\gamma} \right)^{\frac{1}{1-\gamma}} \tag{C.5}$$

$$\sum_{k \in \mathcal{G}} (1 - \alpha_k) X_i^k = w_i^l N_i^l \tag{C.6}$$

$$X_i^M = w_i^M N_i^M \tag{C.7}$$

$$P_j^k = \left(\sum_{i \in \mathcal{L}} \left(\frac{(r_i^k)^{\alpha_k} (w_i^A)^{1-\alpha_k} \kappa_{ij}}{z_i^k c_k} \right)^{1-\eta_k} \right)^{\frac{1}{1-\eta_k}}, \text{ for } k \in \mathcal{K} \tag{C.8}$$

$$P_j^M = \left(\sum_{i \in \mathcal{L}} \left(\frac{w_i^M \kappa_{ij}}{z_i^M} \right)^{1-\eta_M} \right)^{\frac{1}{1-\eta_M}} \tag{C.9}$$

$$N_j^s = \sum_{lt=\theta(ik,js)} \{ \Phi_i(m_{ik}^{\kappa(ik,lt+1)}) - \Phi_i(m_{ik}^{\kappa(ik,lt)}) \} \frac{(E_j^s / P_{js})^{\nu} (m_{ik}^{js})^{-\nu}}{\sum_{j's'=1}^{lt} (E_{\kappa(ik,j's')} / P_{\kappa(ik,j's')})^{\nu} (m_{ik}^{\kappa(ik,j's')})^{-\nu}} N_i^{k,0} \tag{C.10}$$

$$r_i^k = \frac{\alpha_k X_i^k}{\phi^i A_k^i (\pi_k^i)^{\frac{\theta-1}{\theta}}}, \text{ for } k \in \mathcal{K} \tag{C.11}$$

$$\pi_i^k = \frac{(r_i^k A_i^k)^{\theta}}{\sum_{p \in \mathcal{K}} (r_i^p A_i^p)^{\theta}}, \text{ for } k \in \mathcal{K} \tag{C.12}$$

$$E_j^s = w_j^s + R_j^s / N_j^s \tag{C.13}$$

To compute the equilibrium, we inspire from the method of Conte (2022). With a guess for X_i^k, we solve for r_i^k and π_i^k with equations (C.11) and (C.12), using a guess for r_i^k. Then, we solve for optimal population distribution and wages with equation (C.10), (C.6), (C.7) and (C.13), using a guess for N_i^s and a guess for w_i^s. We then solve for the optimal price index and share of consumption using equations (C.3), (C.5), (C.8), (C.9), (C.13) and (C.4), using a guess for P_j. Finally, we solve for the optimal value of production with equations (C.1) and (C.2). We iterate on this algorithm until convergence.

C.2 Inversion of the model

C.2.1 Production

To calibrate the model on real data on production and population distribution, we need to invert the model. We take the equations of the spatial equilibrium (section C.1) and change them to retrieve the fundamentals of the model $\{z_i^k, \Omega_k\}$, given the following variables $\{X_i^k, N_j^s\}$. The equations defining the inversion of the model are presented below:

$$z_i^k = \left(\frac{1}{X_i^k} \sum_{j \in \mathcal{L}} \left(\frac{(r_i^k)^{\alpha_k} (w_i^l)^{1-\alpha_k} \kappa_{ij}}{c_k P_j^k} \right)^{1-\eta_k} (P_j^k / P_j^A)^{1-\gamma} \left(\mu_{jA}^A E_j^A N_j^A + \mu_{jM}^A E_j^M N_j^M \right) \right)^{\frac{1}{1-\eta_k}} \tag{C.14}$$

$$z_i^M = \left(\frac{1}{X_i^M} \sum_{j \in \mathcal{L}} \left(\frac{w_i^M \kappa_{ij}}{P_j^M} \right)^{1-\eta_M} \left(\mu_{jA}^M E_j^A N_j^A + \mu_{jM}^M E_j^M N_j^M \right) \right)^{\frac{1}{1-\eta_M}} \tag{C.15}$$

$$\frac{\Omega_A}{\Omega_M} = \frac{X_A}{X_M} \frac{\sum_{i \in \mathcal{L}} \sum_{j \in \mathcal{L}} \left(\frac{w_i^M \kappa_{ij}}{z_i^M P_j^M} \right)^{1-\eta_M} \left(\left(\frac{P_j^M}{P_{jA}} \right)^{1-\sigma} \left(\frac{E_j^A}{P_{jA}} \right)^{\epsilon_M - (1-\sigma)} E_j^A N_j^A + \left(\frac{P_j^M}{P_{jM}} \right)^{1-\sigma} \left(\frac{E_j^M}{P_{jM}} \right)^{\epsilon_M - (1-\sigma)} E_j^M N_j^M \right)}{\sum_{k \in \mathcal{K}} \sum_{i \in \mathcal{L}} \sum_{j \in \mathcal{L}} \left(\frac{(r_i^k)^{\alpha_k} (w_i^A)^{1-\alpha_k} \kappa_{ij}}{z_i^k c_k P_j^k} \right)^{1-\eta_k} (P_j^k / P_j^A)^{1-\gamma} \left(\left(\frac{P_j^A}{P_{jA}} \right)^{1-\sigma} \left(\frac{E_j^A}{P_{jA}} \right)^{\epsilon_A - (1-\sigma)} E_j^A N_j^A + \left(\frac{P_j^A}{P_{jM}} \right)^{1-\sigma} \left(\frac{E_j^M}{P_{jM}} \right)^{\epsilon_M - (1-\sigma)} E_j^M N_j^M \right)} \tag{C.16}$$

$$w_i^A = \frac{\sum_{k \in \mathcal{G}} (1 - \alpha_k) X_i^k}{N_i^A} \tag{C.17}$$

$$w_i^M = \frac{X_i^M}{N_i^M} \tag{C.18}$$

$$r_i^k = \frac{\alpha_k X_i^k}{\phi^i A_k^i (\pi_k^i)^{\frac{\theta-1}{\theta}}} \text{ , for } k \in \mathcal{K} \tag{C.19}$$

$$\pi_i^k = \frac{(r_i^k A_i^k)^\theta}{\sum\limits_{p \in \mathcal{K}} (r_i^p A_i^p)^\theta} \text{ , for } k \in \mathcal{K} \tag{C.20}$$

To solve this system of nonlinear equations, we first retrieve factor prices using equations (C.17), (C.17), (C.19) and (C.20), using a guess for r_i^k. Then, we use a guess for z_i^k and Ω_k. We solve for price indexes and shares of consumption with equations (C.3), (C.5), (C.8), (C.9), and (C.4), using a guess for P_j. Then, we solve for z_i^k and Ω_k with equations (C.16), (C.14) and (C.15). We iterate on this algorithm until convergence.

C.2.2 Location choice

Given the vector of wages computed in the previous step, the distribution of population, and the bilateral migration data between location-sector, $\{v_j^s, N_j^s, \beta_{ik}^{js}\}$, we calibrate the migration cost m_{ik}^{js} with the following equation:

$$m_{ik}^{js} = \left(\frac{1}{\beta_{ik}^{js}} \sum_{lt = \theta(ik,js)} \{ \Phi(m_{ik}^{\kappa(ik,lt+1)}) - \Phi(m_{ik}^{\kappa(ik,lt)}) \} \frac{(E_j^s / P_{js})^\nu}{\sum_{j's'=1}^{lt} \left(E_{\kappa(ik,j's')} / P_{\kappa(ik,j's')} \right)^\nu (m_{ik}^{\kappa(ik,j's')})^{-\nu}} \right)^{1/\nu} \tag{C.21}$$

To solve this system of nonlinear equations, we start with a guess for m_{ik}^{js} and solve for m_{ik}^{js} with equation (C.21), until convergence.

C.3 Migration costs

We compare our calibrated migration costs with those obtained in other studies. Here, we focus only on internal migration costs.

Method of Tombe and Zhu (2019) The equation of migration of the model gives:

$$\pi_{i,j} = \frac{\left(w_s^j / P_j\right)^{\nu} \left(m_s^{i,j}\right)^{-\nu}}{\sum_{q \in Q} \left(w_s^q / P_q\right)^{\nu} \left(m_s^{i,q}\right)^{-\nu}} \tag{C.22}$$

which yields the following share of migrants relative to the number of non-migrants at the origin:

$$\frac{\pi_{i,j}}{\pi_{i,i}} = \left(\frac{w_j}{w_i m_{i,j}}\right)^{\nu} \tag{C.23}$$

We invert this equation using data used to calibrate our model: GDP per capita data from Rossi-Hansberg and Zhang (2025), bilateral migration data from Ceausu et al. (2021), and $\nu = 3$ from Morten and Oliveira (2024).

Method of Conte (2022) We compute the distance between each administrative unit's main city in our model using data on road networks. We then set migration costs to be equal to:

$$m_{i,j} = m_{c_j} distance(i,j)^{\phi}, \text{ with } \phi = 0.46 \tag{C.24}$$

As calibrated data on country barriers are not accessible, we compare migration cost estimates only for internal migration.